NATIONAL AERONAUTICS AND SPACE ADMINISTRATION

Space Programs Summary 37-41, Vol. VI

Space Exploration Programs and Space Sciences

For the Period July 1 to August 31, 1966

GPO PRICE $ _____

CFSTI PRICE(S) $ _____

Hard copy (HC) ___*3 0 0*___

Microfiche (MF) ___*65*___

ff 653 July 65

JET PROPULSION LABORATORY

CALIFORNIA INSTITUTE OF TECHNOLOGY

PASADENA, CALIFORNIA

September 30, 1966

Space Programs Summary 37-41, Vol. VI

Space Exploration Programs and Space Sciences

For the Period July 1 to August 31, 1966

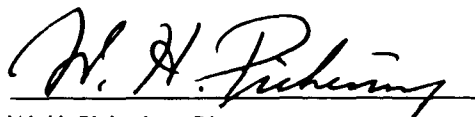Space Programs Summary 37-41, Vol. VI

Preface

The Space Programs Summary is a six-volume bimonthly publication designed to report on JPL space exploration programs and related supporting research and advanced development projects. The titles of all volumes of the Space Programs Summary are:

Vol. I.   *The Lunar Program* (Confidential)

Vol. II.   *The Planetary–Interplanetary Program* (Confidential)

Vol. III. *The Deep Space Network* (Unclassified)

Vol. IV.   *Supporting Research and Advanced Development* (Unclassified)

Vol. V.   *Supporting Research and Advanced Development* (Confidential)

Vol. VI.   *Space Exploration Programs and Space Sciences* (Unclassified)

The Space Programs Summary, Vol. VI, consists of: an unclassified digest of appropriate material from Vols. I, II, and III; an original presentation of the JPL quality assurance and reliability efforts, and the environmental- and dynamic-testing facility-development activities; and a reprint of the space science instrumentation studies of Vols. I and II. This instrumentation work is conducted by the JPL Space Sciences Division and also by individuals of various colleges, universities, and other organizations. All such projects are supported by the Laboratory and are concerned with the development of instruments for use in the NASA space flight programs.

Approved by:

W. H. Pickering, Director
Jet Propulsion Laboratory

Contents

LUNAR PROGRAM

PLANETARY–INTERPLANETARY PROGRAM

DEEP SPACE NETWORK

Contents (contd)

SPACE SCIENCES

SUPPORTING ACTIVITIES

I. Surveyor Project

LUNAR PROGRAM

A. Introduction

The *Surveyor A-21* model flight spacecraft are designed to span the gap between the *Ranger* Project and the *Apollo* Project by making soft landings on the Moon to extend our knowledge of lunar conditions and determine the suitability of sites for proposed *Apollo* spacecraft landings. The engineering payload includes elements of redundancy, diagnostic telemetry, touchdown instrumentation, and survey TV.

Surveyor I, the first flight spacecraft, was launched from Cape Kennedy, Florida, on May 30, 1966, and soft-landed on the Moon on June 2, 1966. By June 14, when lunar sunset occurred, approximately 100,000 commands had been received by the spacecraft, and 10,338 pictures of the spacecraft and its immediate vicinity had been transmitted.

Editorial note: After the close of the reporting period (July 1 to August 31, 1966), the second flight spacecraft, Surveyor II, was launched from Cape Kennedy on September 20. The spacecraft responded well until the command was given for midcourse thrust execution. At that time, one vernier engine did not ignite, and the

spacecraft began to tumble. Numerous attempts to correct the problem were unsuccessful, and the spacecraft impacted the lunar surface at approximately 03:18 GMT on September 23. The Surveyor II launch and mission operations and plans for the third launch, currently scheduled for the first quarter of 1967, will be covered in SPS 37-42, Vol. VI.

Hughes Aircraft Company (HAC), Space Systems Division, is under contract to fabricate the *Surveyor A-21* spacecraft. The launch vehicle, a combination *Atlas/ Centaur*, is provided by General Dynamics/Convair. Control, command, and tracking functions for the *Surveyor* missions are performed by the JPL Deep Space Network and Missions Operations System.

B. Surveyor I Mission Operations and Subsystem Performance

1. Mission Operations

The first lunar sunset for *Surveyor I* occurred on June 14. The spacecraft survived the conditions of lunar night and, in its second lunar day, was reactivated by the

Tidbinbilla Deep Space Station (DSS 42) at 11:29:10 GMT on July 6. The first good data frame was received approximately 7 min later. At 11:40:36, all spacecraft currents began to increase with an initial rate of 20% of full scale/min. About 5 min later, the currents reached full-scale limits. Intermittent loss of lock on the telemetry link was experienced. The current started decreasing 23 min later. At 12:23:26, normal levels were reached and the current remained steady from then on. The command link to the spacecraft was lost.

At 12:25 on Earth, the decision was made to go to two-way lock. Two-way lock was obtained, and, at 13:15, solar panel stepping was initiated. Main battery voltage was about 17 v, and occasional loss of up- and down-link lock was encountered. After a few attempts at solar panel stepping, the unregulated bus voltage rose to normal. Battery charge current became positive and rose to 1 amp (net); discharge dropped to zero. After 30 min of assessment, stepping was resumed in roll, solar panel, and planar array to get the planar array pointed to Earth without appreciably moving the solar panel off the Sun. After this was accomplished, operations were switched to the 1100-bits/sec mode. Final signal strength was −117.4 dbm.

Due to the available battery charge rate of only 1 amp when transmitting in lower power, it was decided to shut the spacecraft down for 2-hr periods to allow charging "in the blind." Short interrogations were scheduled at 2-hr intervals. By this load reduction, it was hoped that the battery charge rate would nearly double. At 00:02 GMT on July 7, the spacecraft was shut down. Turn-on commands issued to the spacecraft at 02:00 resulted in no response. During the entire pass of the Johannesburg DSS (DSS 51), the spacecraft could not be reactivated. Finally, at 08:25, the spacecraft signal was detected by the Pioneer DSS (DSS 11) at a −165-dbm level (extremely weak: some 46 db lower than anticipated for lower-power planar array operation) after 2 hr of search. Transmitter A was commanded off, and the signal disappeared. With the turn-on of Transmitter B, *Surveyor I* returned to a normal condition at expected dbm levels. A telecommunications and signal processing engineering assessment was conducted, and Transmitter A was again commanded on. Its response was as flawless as its previous lunar-day performance at predicted dbm levels. The remainder of the DSS 11 pass was accomplished using Transmitter A, and good-quality 600-line TV pictures were taken. The spacecraft was then shut down and revived by DSS 42 at 21:00. All signals indicated a nominal condition for the spacecraft, and the

battery was charging at a rate in excess of 1 amp. The next interrogation was at 23:30. The above revivals of the spacecraft were unprecedented in either tests or operations.

The spacecraft did not respond to thrust-phase power-on commands to fire the vernier engines at 22:45 GMT on July 8. At 00:00 GMT on July 9, the main battery temperature was 135°F and was increasing to its survival temperature limit of 142°F at the rate of approximately 1°F/hr. At approximately 05:00 on July 9, the spacecraft was put in a noncharging quiescent mode; i.e., only the receivers were left on. Main battery temperature at this time was 139.8°F. After several hours, it became apparent that this temperature was stabilizing. At 16:00, battery recharging was commenced at a quiescent charge rate of about 1.25 amp. The solar panel was positioned approximately 24 deg from the vertical toward the east when battery recharging was begun. About 12 hr later, the charge rate was increased to about 2 amp in the quiescent mode. The panel was positioned an additional 36 deg from the vertical toward the east when the charge rate was increased. Main battery temperature continued to drop and stabilized at about 112°F on July 11. A reversal phenomenon whereby the main battery pressure decreased during charging of the battery and increased during discharging of the battery is being analyzed. During operations on July 9 and 10, Transmitter A intermittently failed to respond to turn-on commands.

The survey TV camera was operated periodically during the DSS 11 pass, and eight TV interrogations of approximately 1 hr each were performed. The transfer from DSS 11 to DSS 42 took place between 20:46 and 20:56 GMT on July 12. Spacecraft performance appeared normal. The DSS 42 and DSS 51 TV picture-taking sequences were such that spacecraft shadow effects could be observed.

At 22:00 GMT on July 13, DSS 11 again acquired *Surveyor I* and TV pictures were taken. The solar panel was in a near-vertical position, tilted approximately 3 deg toward the west. Just prior to lunar night, the solar panel was stored in a 20-deg westerly tilt from the vertical to cast a long shadow for the *Lunar Orbiter* spacecraft at NASA's request.

At approximately 02:45 GMT on July 14, communications with *Surveyor I* failed. Nine pictures of the sunset sequence had been taken. Upon the start of the tenth

TV frame, no response was received to the start command issued by DSS 51. When commands were sent to turn survey power off, turn high voltage off, and transfer switch to lower power, all contact was lost. No response was indicated to a frequency search of ± 20 kc. Other attempts at interrogation all failed. At 08:32 GMT on July 14, JPL indicated to all deep space stations that they were no longer required to support *Surveyor I* lunar operations.

2. Propulsion Subsystem Performance

The total *Surveyor I* velocity decrement produced jointly by the retrorocket engine and the vernier engines was 8410 ft/sec, as compared to the nominal 8440 ft/sec. The maximum deceleration produced during the retrorocket firing period was 9.85 g, as compared to the predicted value of 9.82 g. Analysis of the vernier engine thrust data indicates that the roll moment generated by the retrorocket engine was almost nonexistent and that alignment of the retrorocket engine thrust vector to the spacecraft center of gravity was within 0.013 in., as opposed to the 0.18-in. specification allowance. Data reduction with regard to establishment of the actual retrorocket firing time is still in progress. Efforts to date indicate that the retrorocket burned about 1% longer than the in-flight prediction of 38.5 sec. This 1% deviation was greater than anticipated, but was well within the system capability of the spacecraft.

3. Flight-Control Subsystem Performance

During the *Surveyor I* mission, a new technology was demonstrated: for the first time, it was possible to measure the drift of gyros in a 0-g field by use of the *Surveyor I* flight-control subsystem. This was made possible by the combination of a gyro inertial reference with a completely independent celestial inertial reference (Sun and star) and the capability of the flight-control subsystem to operate using either reference.

By caging the gyro reference and the vehicle attitude to the Sun and Canopus sensors and then switching the attitude-control subsystem to the uncaged gyro reference, the vehicle attitude followed the gyro drift; at the same time, the Sun and star reference system was monitored by telemetering. The Sun and star error signals indicated the gyro drift. Evaluation of these data during the mission (with several measuring periods averaging 2 hr each) resulted in a good check of the gyro drift. With a known gyro drift rate, it was possible to intentionally bias the preretromaneuvers to allow for gyro

drift, resulting in more accurate vehicle pointing. This drift compensation was included in plans for the mission and helped assure the success of the *Surveyor I* terminal descent.

4. Temperature-Control Subsystem Performance

The *Surveyor I* temperature-control subsystem provided temperatures throughout transit that were close to predictions. On the average, the temperatures were consistent with a Sun intensity on the low side of nominal, as defined by the solar intensities in the HAC solar-thermal-vacuum chamber. Preflight predictions were prepared for the 72 temperature sensors carried on the spacecraft, and all but four of the in-flight temperatures were within the prediction band.

Temperature predictions were not prepared for the lunar-surface phase of the mission. The temperatures during this phase were highly dependent upon the roll orientation of the spacecraft. The compartment system performed better than expected during the lunar day. Preliminary analysis indicates that the total environmental lunar-noon heat inputs to the compartment radiators were approximately 30% less than anticipated. The difference appears to be due to lower-than-anticipated temperatures on the solar panel, planar array antenna, and spaceframe.

With the onset of lunar night, anomalous thermal switch performance was observed. Several of the compartment switches did not open, even at temperatures considerably below the design opening temperature. Second-lunar-day temperature data indicated that all the switches eventually opened; however, this conclusion was based on analysis and is therefore subject to question. TV inspection of the spacecraft during the second lunar day showed that one quadrant of a thermal switch radiator on Compartment A had been shattered. This apparently was the result of the extremely low temperatures ($-300°F$) experienced during the lunar night. However, the damaged radiator had no noticeable effect on the performance of the spacecraft.

C. Systems Testing and Assembly

1. SC-2 (Second Flight Spacecraft) Flight-Acceptance Tests

As reported in *SPS 37-40*, Vol. VI, p. 8, during the terminal-descent portion of the SC-2 solar-thermal-vacuum Phase 1C mission sequence, the boost regulator

failed, causing a loss of power to the spacecraft. Tests revealed that the problem was inherent in the regulator, and the unit was subsequently modified to ensure that the failure would not recur. The radar altimeter and doppler velocity sensor (RADVS), signal data converter, and klystron power supply modulator units were replaced as a result of excessive thermal stress caused by the RADVS remaining on for a period after the boost regulator failure.

To test the replaced units, a Phase 2C test was performed. This test, run at 100% solar intensity, consisted of: (1) the first 7.5 hr of a normal mission, (2) 6.5 hr of thermal preconditioning to bring the spacecraft to the thermal conditions expected at terminal descent, (3) a terminal-descent sequence beginning 3 hr prior to touchdown, and (4) a special 6-hr TV test. No serious problems were encountered, and the spacecraft was then prepared for vibration tests.

The vibration testing was performed from June 29 to July 10. An examination of the test control accelerometer responses showed close similarity between those of SC-2 and SC-1. On July 4, as the random vibration control level was being set for another run (4B), a severe transient pulse occurred which delivered a shock-type input to the spacecraft. An intensive investigation failed to reveal the source of this transient. As a result, two protective circuits were added. Structural investigation revealed a broken retrorocket support strut and fitting, plus misalignments of the spacecraft retrorocket attach fittings. The retrorocket, support struts, and attach fittings were subsequently changed.

A nonscheduled ¼-g sinusoidal vibration test and a system-readiness test were then conducted to check spacecraft condition before returning to flight-acceptance-test vibration levels. The Phase 4A sinusoidal flight-acceptance test was then repeated. The spacecraft functional and dynamic responses were found to be essentially unchanged from patterns demonstrated prior to the shock-pulse incident. Following a satisfactory random vibration equalization run, the scheduled Phase 4B test (combining sine and random input normal to one leg of the spacecraft) was completed.

The initial phases of test operations for vernier engine vibration were begun July 10. Because of the schedule delay resulting from the shock transient delivered during boost level vibration, it was decided to forego ballasting the vernier propulsion system. The "dry-run" terminal descent was unsuccessful due to a failure traced to a crystal

in the RADVS system. This system was removed and shipped to the vendor for rework, and RADVS components were borrowed from SC-3 (third flight spacecraft). The vibration facility was converted to accomplish a special sine vibration transmissibility test. The RADVS system was reassembled, and the dry-run terminal descent was successfully completed. The closed-loop midcourse correction, the closed-loop terminal descent, and the RADVS search mode tests were also completed without difficulty, thus concluding vibration testing on July 13.

The SC-2 spacecraft was shipped to the Eastern Test Range (ETR) on July 18. Following thermal finish rework at the end of its testing at HAC, the spacecraft had been cleaned using the special vacuum cleaning techniques developed during *Surveyor I* (SC-1) operations. These same cleaning operations were scheduled to be repeated just prior to encapsulation of SC-2 for launch at the ETR. After its arrival at the ETR, SC-2 was transported to the spacecraft checkout facility. The removal of SC-2 from its ground transport vehicle is shown in Fig. 1. The antenna/solar panel positioner was found to have sprung open in flight; however, a detailed inspection and a special test revealed no damage to the unit.

Initial ETR operations included receiving inspection, spacecraft assembly, and performance verification tests. After these operations were completed, the spacecraft was transported to the explosive safe area on August 2. Here SC-2 underwent preparations for joint flight-acceptance composite testing. These preparations were completed with a system-readiness test on August 9, at which time the encapsulated spacecraft was transported to the launch complex and mated with the *Atlas/Centaur 7* launch vehicle for the scheduled 9-day joint flight-acceptance composite test.

2. SC-3 (Third Flight Spacecraft) Flight-Acceptance Tests

Initial system checkout was completed July 15, except for the checkout of mechanisms and telecommunications. The following day marked the beginning of preparations for the mission-sequence/electromagnetic-interference test phase. Problems encountered during these preparations necessitated replacement of the transmitter and the engineering signal processor. The first sequence of the test phase, begun July 24, consisted of a system-readiness test and a non-real-time mission sequence at a stepped voltage input. This sequence was completed July 27, with the only serious problem encountered
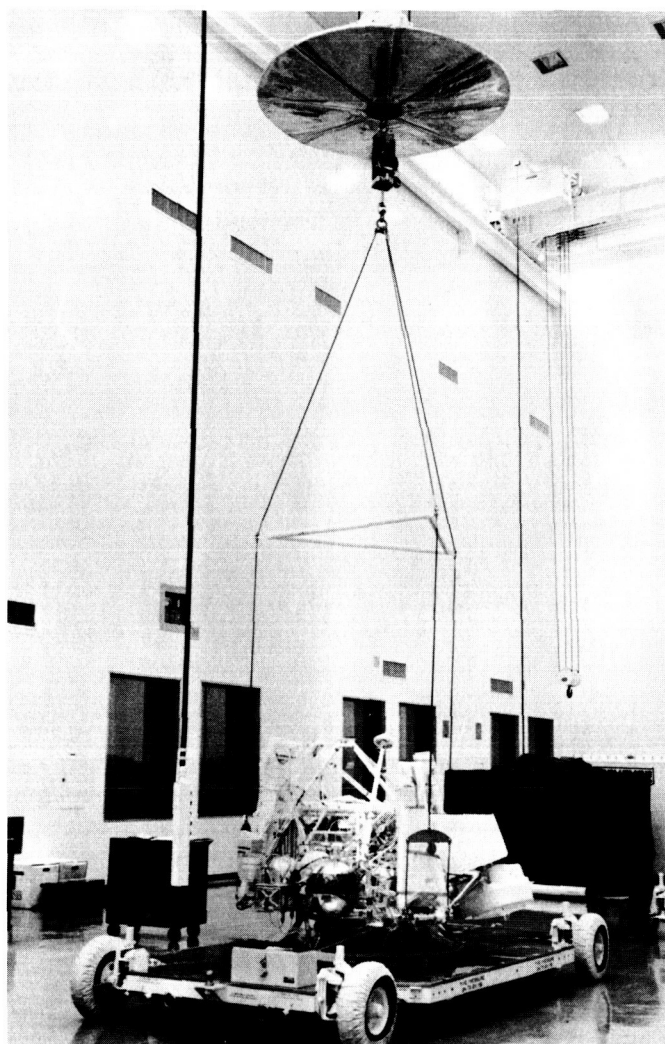
Fig. 1. Removal of SC-2 from its ground transport vehicle at the ETR spacecraft checkout facility

being a failure of a battery charge regulator. After replacement of the regulator, the second and third sequences of the test phase were completed. The third sequence was a real-time mission sequence under electromagnetic-interference conditions. After its completion on August 6, the mission-sequence/electromagnetic-interference test phase was considered completed, and preparations for solar-thermal-vacuum testing were begun.

Several studies were made concerning additional payloads for both the SC-3 and SC-4 flight spacecraft. One concerned the addition of a stripped-down version of a soil mechanics surface sampler. A retrofit kit would consist of a substructure assembly to modify the existing TV bracketry to support the surface sampler and a sup-

port bracket for an externally mounted surface sampler electronics auxiliary. The existing TV harness would supply the required power and signal leads. Since no harness or compartment would be required, a last-minute decision concerning this installation can be made. Another study concerned the addition of two planar mirrors to the lower part of the spacecraft to permit one of the TV cameras to view the crushable blocks and thrust chamber assemblies to evaluate crushing or impingement into the lunar surface after landing.

3. SC-4 (Fourth Flight Spacecraft) Flight-Acceptance Tests

Preparation for telecommunications integration of SC-4 on the system test stand began July 14. Telecommunications integration was initiated July 20, but was stopped 2 days later when several units were removed for use on SC-3. This integration effort was later completed, and integration of the flight-control/telecommunications systems was initiated. Solar-thermal-vacuum testing of SC-4 should begin during the next reporting period.

4. SC-5, SC-6, and SC-7 (Fifth, Sixth, and Seventh Flight Spacecraft) Assembly

The SC-5 basic spaceframe was completed and is in the final assembly area for substructure installation. This is scheduled for completion during the next reporting period. The SC-6 basic spaceframe is nearing completion, and assembly of the SC-7 spaceframe has begun. All engineering associated with these vehicles has been completed.

D. Electrical Power Source

The production of type-approval hardware for the solar panels for SC-5 through SC-7 has been initiated. As reported in *SPS 37-40*, Vol. VI, p. 11, the new design differs from that of SC-1 through SC-4 in that it incorporates the flat solar cell mounting technique rather than the rigid shingle concept. The design prototype panel (developmental panel) has been fabricated and environmentally tested. Fig. 2 shows the partially cell-covered panel mounted in its specially designed handling frame. The developmental panel has approximately the same dimensions as the flight solar panels, the one major difference being that the developmental panel has a honeycomb of $3/8$-in. thickness whereas the flight panel will have a honeycomb of $1/2$-in. thickness. To evaluate the effect of environmental testing on the cells, four sections of series-connected submodules were bonded to the
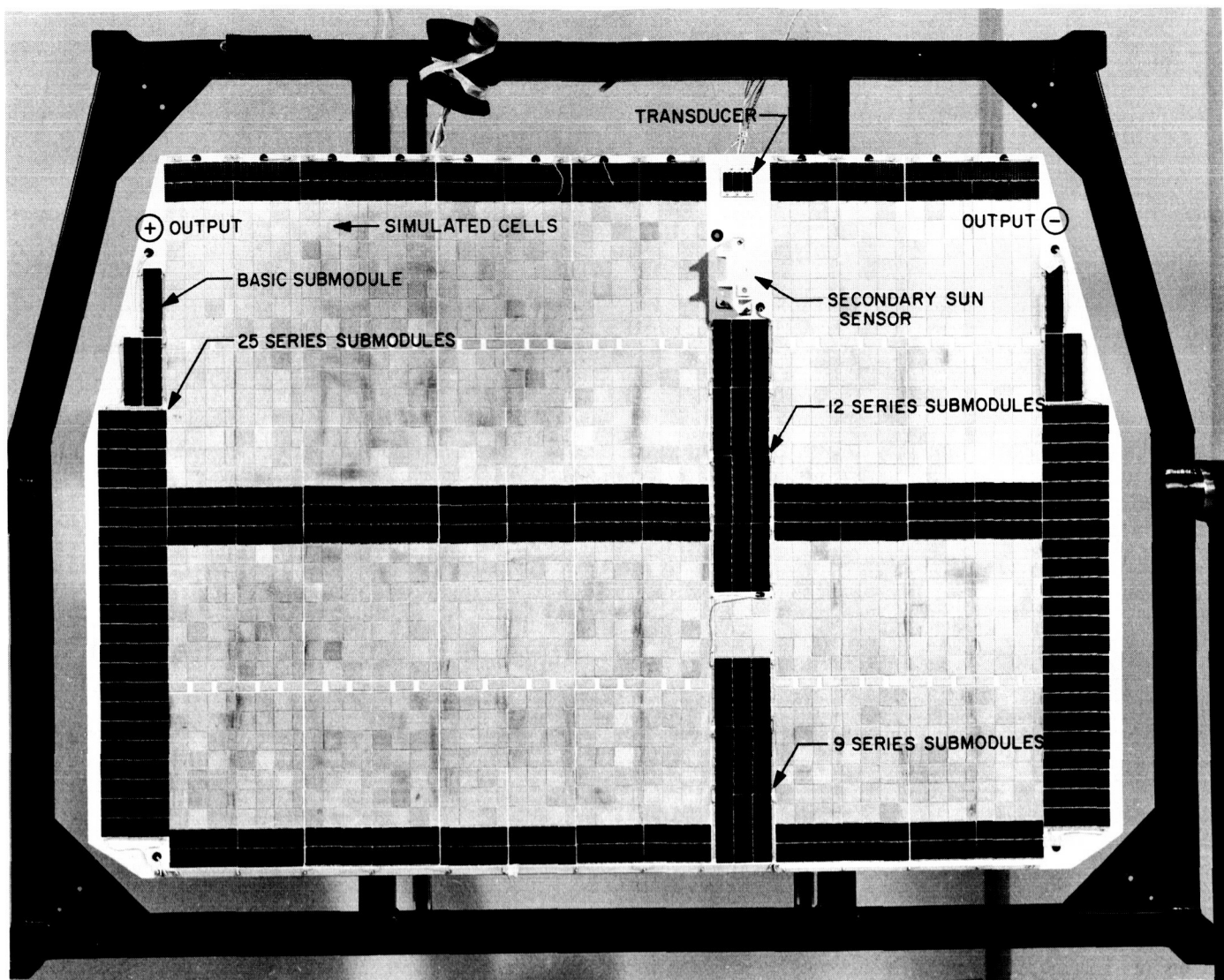
Fig. 2. Developmental solar panel mounted in handling frame

developmental panel in a strategic section of the panel, and the panel was subjected to a type-approval environmental test program. Aluminum blanks were bonded to the remaining cell surface area of the panel to simulate the mass loading of a completely celled panel.

Before and after each test, the panel underwent sunlight electrical performance testing. The results of these tests indicated that the panel suffered no detectable degradation due to exposure to the vibration, humidity, or acoustic environments. Approximately 3% maximum power degradation was detected, however, after the panel was exposed to the high-temperature thermal-vacuum environment. This level agrees very well with

that of similar solar cells of another test program which were measured after a similar high-temperature, long-term exposure. It is not anticipated that the panel will experience degradation due to exposure to expected flight temperatures.

E. Flight Control

A star sensor window-fogging problem was observed during SC-1 and SC-2 solar-thermal-vacuum testing. Subsequently, both thermal and thermal-vacuum tests on individual Canopus sensors were made, and chemical analyses of window deposits were accomplished. It was determined that fogging of the window was due to the

vaporization of various lubricants when the sensor was at a high internal operating temperature and the subsequent deposition of the vapors on the inside of the star sensor window which is exposed to the cold space environment. Analyses of window deposits indicate that 90% of the deposited material is from the silicone vacuum grease applied to the O-ring that seals the star sensor window to the sensor body. The balance of the deposit is from gear lubricants, volatile materials in motor windings, and other sources. To eliminate the deposits, it was necessary to reduce the temperature differential between the interior of the unit and the inner surface of the star window. Among the methods tested, a modification of the paint pattern on the star sensor window light shield provided the largest decrease in temperature differential and was simplest and fastest to implement.

Based on these tests and analyses, it was recommended that the Canopus sensor used on SC-2 be reworked to incorporate a modified paint pattern on the light shield and the window be cleaned and reinstalled, using a dry O-ring. It was further recommended that a Sun channel filter be selected that will yield a 10 to 20% increase in the apparent brightness of Canopus to provide a Canopus lock-on signal, even with the extremely unlikely possibility of degradation due to window fogging.

F. Spacecraft Mechanisms

As reported in *SPS 37-40*, Vol. VI, pp. 7, 8, the *Surveyor I* omnidirectional antenna A failed to extend at the spacecraft's separation from the *Centaur* stage, but later extended after touchdown on the lunar surface. Antenna performance data received later confirmed that extension had actually taken place. The failure was attributed to excessive friction at the pinpuller mechanism interface and at the area of the pivot bearing.

The omnidirectional antenna A and B mechanisms use tapered fiberglass cloth tubes bonded to aluminum hinge bracket assemblies. Changes for SC-2 resulting from the *Surveyor I* anomaly were of two types: functional improvements and stress improvements. Included were anodizing and dry-film lubrication of certain parts and redesign for a positive stress margin in torsion spring material. A systems-level test has been specified to ensure that the mechanisms are free after omnidirectional antenna alignment and adjustment and that, when the pinpullers are retracted, the mechanism motion in a 1-g field is sufficient to clear the pinpuller fork. A second test was specified to verify the force required to initiate the deployment motion. These tests will demonstrate that the spring forces are proper and that friction levels are acceptable.

II. Mariner Venus 67 Project

PLANETARY—INTERPLANETARY PROGRAM

A. Introduction

The primary objective of the *Mariner* Venus 67 Project is to conduct a flyby mission to Venus in 1967 to obtain scientific information which will complement and extend the results obtained by *Mariner II* relevant to determining the origin and nature of Venus and its environment. Secondary objectives are to: (1) acquire engineering experience in the conversion of a spacecraft designed for a mission to Mars (spare flight spacecraft from *Mariner* Mars 1964 Project) into one designed for a mission to Venus and in the operation of such a spacecraft, and (2) obtain information on the interplanetary environment during a period of increasing solar activity. An *Atlas/Agena D* launch vehicle will be used.

Due to the minimum length of time (18 months) between authorization of the project and the launch opportunity, techniques and hardware developed during prior projects must be utilized to the fullest extent possible. The single flight spacecraft, designated M67-2, will be a converted *Mariner* Mars 1964 Project flight spare. Portions of the proof test model and certain critical spare units from the *Mariner* Mars 1964 Project are being prepared for use as a flight support spacecraft, designated M67-1. The flight support spacecraft will serve the double function of a pseudo-proof test model and a backup spacecraft for qualifying spare subsystems.

Various changes to the *Mariner* Mars 1964 spacecraft design are necessitated by the fact that the M67-2 flight spacecraft will travel toward, rather than away from, the Sun; also, conversions must be made to accommodate the revised encounter sequencing and science payload.

The S-band radio occultation experiment, one of seven scientific experiments approved for the mission, requires the use of only the RF transmission subsystem on the spacecraft. The celestial mechanics experiment uses only the tracking doppler data derived from the RF carrier. The ultraviolet photometer, helium magnetometer, solar plasma probe, and trapped radiation detector experiments are to be accomplished using existing instrumentation with only minor modifications. Only the dual-frequency radio propagation experiment requires the incorporation of a new scientific instrument into the payload. The Principal Scientific Investigators for these experiments are given in Table 1.

During this reporting period, the spacecraft detail design phase was essentially completed, and emphasis has now shifted toward the actual testing and validation of the design. A parametric analysis concerning the actual probability of contaminating the planet Venus by impacting it with the launch vehicle, the spacecraft, or ejecta from the spacecraft was also completed. NASA

Table 1. Mariner Venus 67 Principal Scientific Investigators

Experiment	Principal Scientific Investigator	Affiliation
S-band radio occultation	A. J. Kliore	Jet Propulsion Laboratory
Ultraviolet photometer	C. A. Barth	University of Colorado
Dual-frequency radio propagation	V. R. Eshleman	Stanford University
Helium magnetometer	E. J. Smith	Jet Propulsion Laboratory
Solar plasma probe	H. S. Bridge	Massachusetts Institute of Technology
Trapped radiation detector	J. A. Van Allen	State University of Iowa
Celestial mechanics	J. D. Anderson	Jet Propulsion Laboratory

Headquarters concurred with the JPL recommendation that the planetary quarantine constraint be no smaller than 5×10^{-4}.

B. Testing Operations

1. Structural Test Model

The spacecraft composite vibration testing of the structural test model has been completed. The spacecraft, subjected to torsional, lateral, and axial axes of vibrational excitation for approximately 3.5 hr, successfully withstood the design ultimate load and structural qualification dynamic loads.

2. Temperature-Control Model

Various modes of the temperature-control-model simulator tests were run at both Earth and Venus intensities. Results indicate that the thermal design of the spacecraft is adequate and that there is sufficient margin to cover any nonstandard operating modes during flight.

3. Solar Panel Structure

A modal vibration test was conducted using a dummy weighted solar panel structure. The test verified the solar panel properties predicted by analysis to a reasonable degree. The discrepancies that existed are at least partially explained by known differences between test parts and the analytic model. Values of damping ratios

at small amplitudes were also measured in the test. The test gave excellent indication of the existence of a highly damped mode that was impossible to excite with two vibration exciters.

4. Gyro Control Assembly

The gyro control assembly for the Mariner Venus 67 flight spacecraft will be one of two existing flight spare units from the Mariner Mars 1964 Project. No modifications were necessary since system constraints applicable to the assembly were not changed and only the existence of out-of-specification components or those now considered unreliable would necessitate any changes. Extensive testing has shown that no components are out-of-specification, and those which no longer are considered preferred parts have been reviewed and their replacement has been waived due to their inaccessibility and the noncritical effect of their failure modes. Comparison of results obtained during the current testing program with those obtained during the Mariner Mars 1964 Project tests shows remarkable gyro stability and no significant change in any area of the assembly tested.

An additional constraint on the Mariner Venus 67 gyro control assembly was the desirability of demagnetizing it to reduce its interaction with the helium magnetometer on the spacecraft, since determination of the magnetic fields of Venus is one of the primary scientific requirements for the mission. It was felt that such demagnetization might affect gyro performance. Demagnetization of the Mariner Mars 1964 proof-test-model gyro control assembly to the flight specification level revealed no significant degradation of performance.

After a voltage heading test, the assembly will undergo system integration tests. After these, the gyro control assembly will be assembled and tested as a part of the Mariner Venus 67 spacecraft.

C. Design and Development

1. Solar Panels

The radiant flux falling on an electronic bay face from the corresponding solar panel is directly proportional to the bay-to-panel form factor and to the solar intensity. For the Mariner Venus 67 mission, the solar intensity at encounter will be approximately twice the maximum Mariner Mars 1964 level. Had the Mariner Mars 1964 solar panel design been retained, the irradiation of the bay face would have increased proportionately. Removal

of the side shielding to cool the bay would have aggravated the problem by exposing more area to the variable radiation from the panels. Thus, to reduce the bay-to-panel form factor, the celled area of the solar panel has been cut back from the spacecraft bus.

2. Thermal Shields

The upper and lower thermal shield blanket configurations have been modified for the *Mariner* Venus 67 spacecraft design. The modified configurations are shown in Fig. 1. The *Mariner* Venus 67 multilayer superinsulation blankets are fabricated from "predimpled" 0.0005-in.-thick mylar, whereas the *Mariner* Mars 1964 blankets were fabricated from hand-"crinkled" 0.00025-in.-thick mylar. The new material is expected to have a lower effective thermal conductivity due to the retention

of thickness in known thermally shorted areas on the spacecraft.

Although the material is twice as thick as that used on the *Mariner* Mars 1964 spacecraft, only half as many layers are used; thus, no weight increase and improved venting capabilities are realized. This new type of construction was successfully demonstrated during the recently completed temperature-control-model and structural-test-model tests.

The use of polished aluminum peripheral shields will be the same as that for the *Mariner* Mars 1964 spacecraft, except that a small shield below the louvers on Bays 3, 5, 7, and 8 will be omitted. Two additional shield designs are those for the attitude-control jets and the trapped radiation detector. These consist of sheet metal
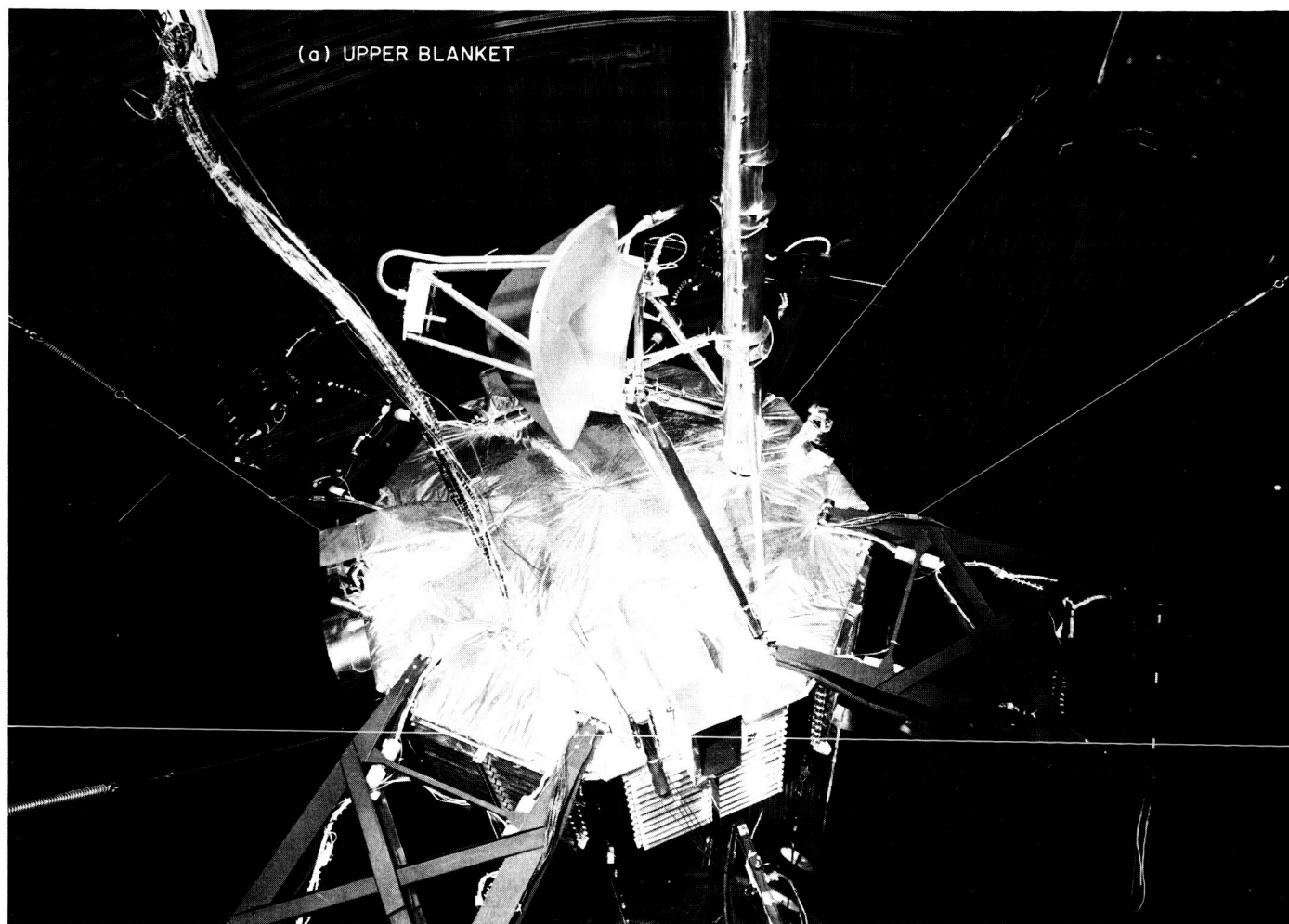

(a) UPPER BLANKET

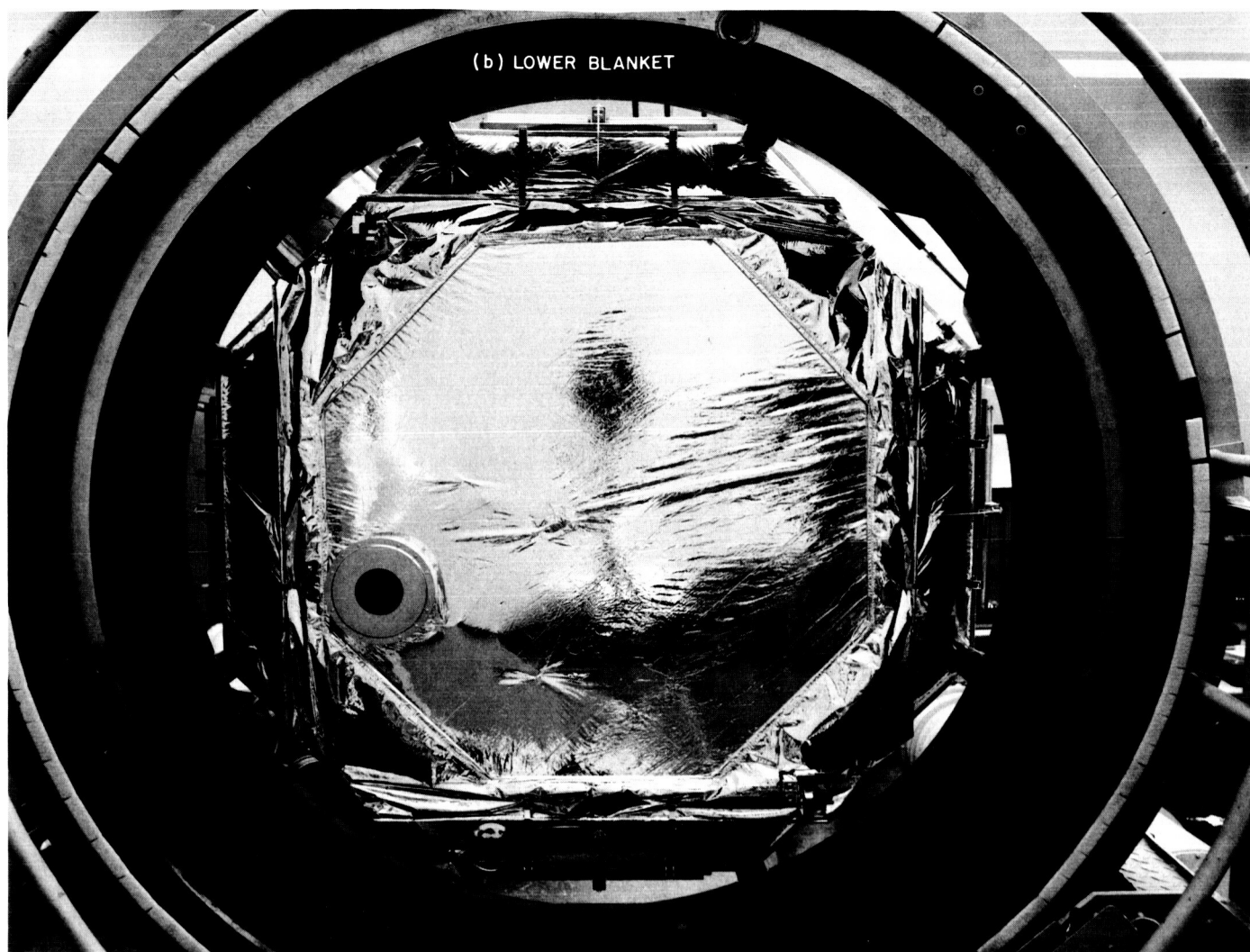Fig. 1. Upper and lower thermal shield blankets

(b) LOWER BLANKET

Fig. 1. Upper and lower thermal shield blankets (contd)

support structures and small multilayer blankets attached to the side of the support structures that will face the Sun. The attitude-control jet shields located on the tips of all four solar panels are similar in design to the Sun shades used on two of the *Mariner* Mars 1964 spacecraft solar panels.

3. Sun Shades

The Sun shade concept and design to be used for the *Mariner* Venus 67 spacecraft are new. Designed to reduce the solar input to the bus by protecting peripheral hardware on the spacecraft from direct sunlight, the shade is composed of a single sheet of 1-mil teflon aluminized on one side, with the teflon side facing the Sun.

During the boost phase, the Sun shade will be retracted to clear the *Agena* adapter and spacecraft interface hardware. Deployed at the same time as the solar panels, the shade will form an octagonal-shaped awning, approximately 10 in. wide, about the periphery of the spacecraft on the sunlit side. The shade in its retracted and deployed positions is shown in Fig. 2.

The new Sun shade has completed thermal type-approval testing on the temperature-control model and structural type-approval testing on the structural test model. Thus far, the temperature-control and structural vibration design objectives have all been achieved. Further tests are planned.

4. Propulsion Subsystem

The design of the *Mariner* Venus 67 propulsion subsystem is identical to that of the *Mariner* Mars 1964 propulsion subsystem, except for a modification of the pyrotechnic cable harness. Like its predecessor, the subsystem will be capable of two starts.

5. Pyrotechnic Subsystem

The *Mariner* Venus 67 pyrotechnic subsystem will have the same degree of redundancy as previous pyrotechnic subsystems. A requirement for repositioning the spacecraft high-gain antenna just before planetary encounter necessitated some rework. The repositioning will be accomplished with a pinpuller identical to those used on the solar panel latches. Two prototype units are being reworked to prove the feasibility of the modification and to gain experience in refabrication of flight-quality units.

The squib initiation circuitry is essentially the same as that used for the *Mariner* Mars 1964 spacecraft. In fact, spare firing units from the *Mariner* Mars 1964 Project will be reworked, retested, and used.
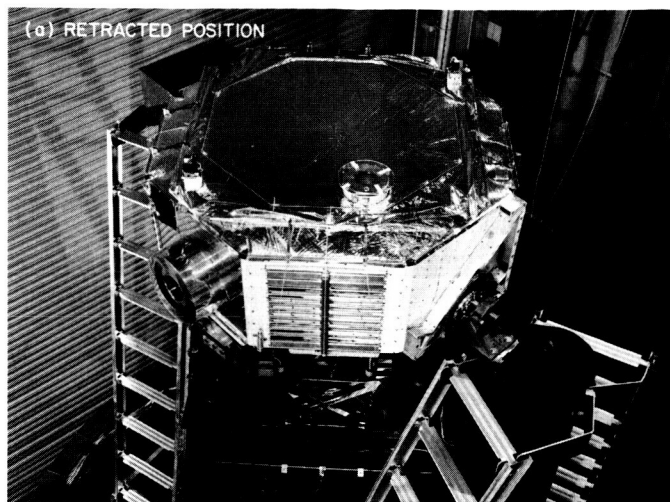

Fig. 2. Sun shade in retracted and deployed positions

III. *Mariner* Mars 1969 Project

PLANETARY—INTERPLANETARY PROGRAM

A. Introduction

The primary objective of the *Mariner* Mars 1969 Project is to conduct two flyby missions to Mars in 1969 to make exploratory investigations of the planet which will set the basis for future experiments—particularly those relevant to the search for extraterrestrial life. The secondary objective is to develop the technology needed for succeeding Mars missions.

The spacecraft design concept will be based on that of the successful *Mariner IV* spacecraft developed under the *Mariner* Mars 1964 Project. However, considerable modifications will be made to meet the 1969 mission requirements and to enhance mission reliability.

The launch vehicle will be the *Atlas/Centaur SLV-3C*. This vehicle, developed under contract for and direction by the Lewis Research Center by General Dynamics/Convair, has a single- or double-burn capability in its second stage and a considerably increased performance rating over the *Atlas D/Agena D* used in the *Mariner IV* mission.

Mariner Mars 1969 missions will be supported by the Eastern Test Range launch facilities at Cape Kennedy, the tracking and data acquisition facilities of the Deep Space Network, and other NASA facilities.

The six planetary-science experiments tentatively selected by NASA (subject to integration capability) for the *Mariner* Mars 1969 missions are the following: TV, infrared spectrometer, ultraviolet airglow spectrometer, infrared radiometer, S-band occultation, and celestial mechanics. Additionally, a planetary-approach-guidance engineering experiment will be incorporated to test the feasibility and flightreadiness of onboard optical sensors and associated data processing techniques necessary for optical approach guidance. The Scientific Investigators for the planetary-science experiments are listed in Table 1.

Selection of contractors for spacecraft subsystems and system design of the spacecraft continued during this reporting period. Most of the functional requirements have been written, but certain problems still exist in evolving a mission and spacecraft design that will satisfy the various experiment requirements.

B. Mission Analysis

Only Type I trajectories will be used for the *Mariner* Mars 1969 missions. The exact trajectories have not yet been defined. A project decision regarding the launch mode (either direct ascent or parking orbit) will be made
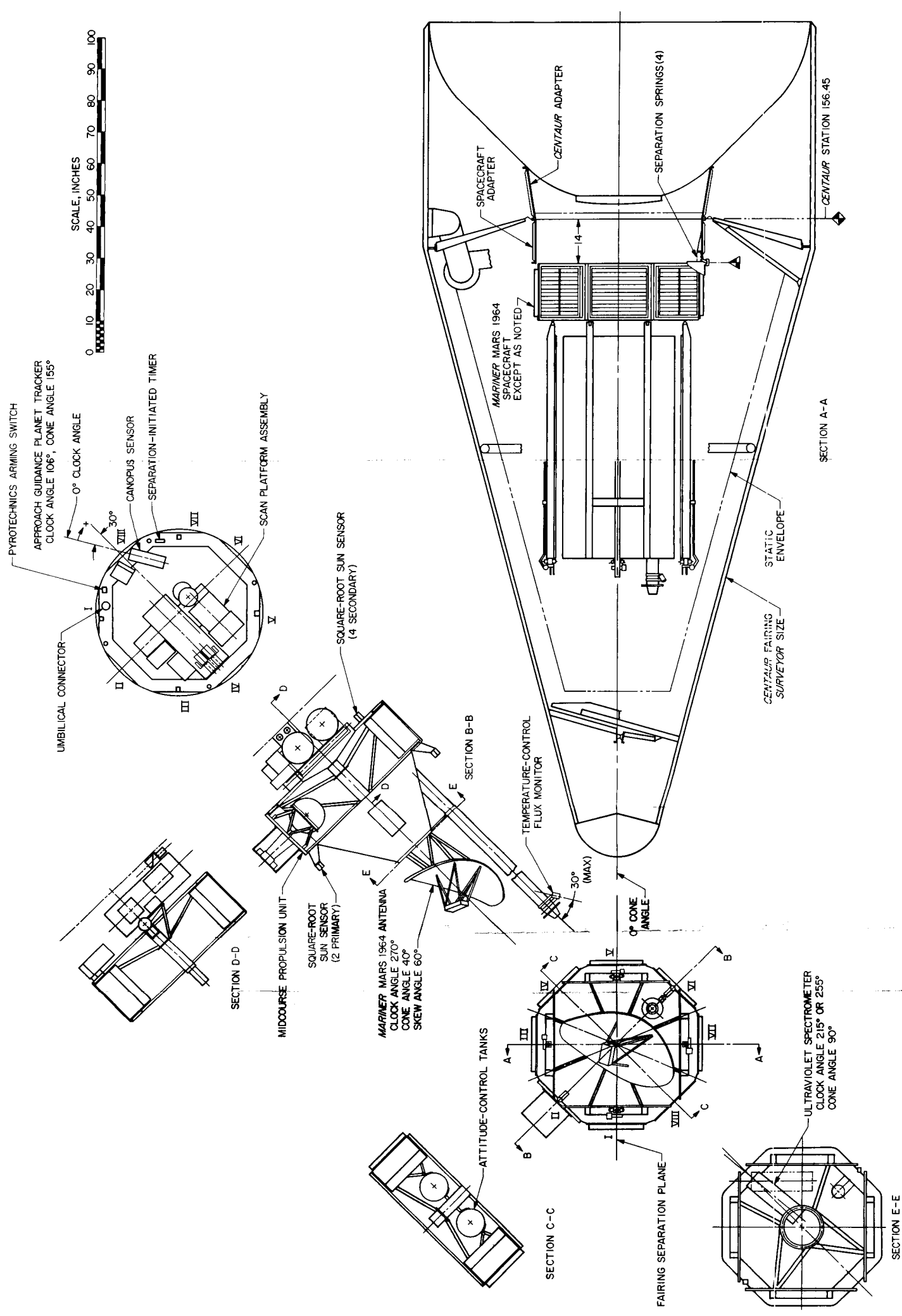
Fig. 1. Mariner Mars 1969 spacecraft configuration

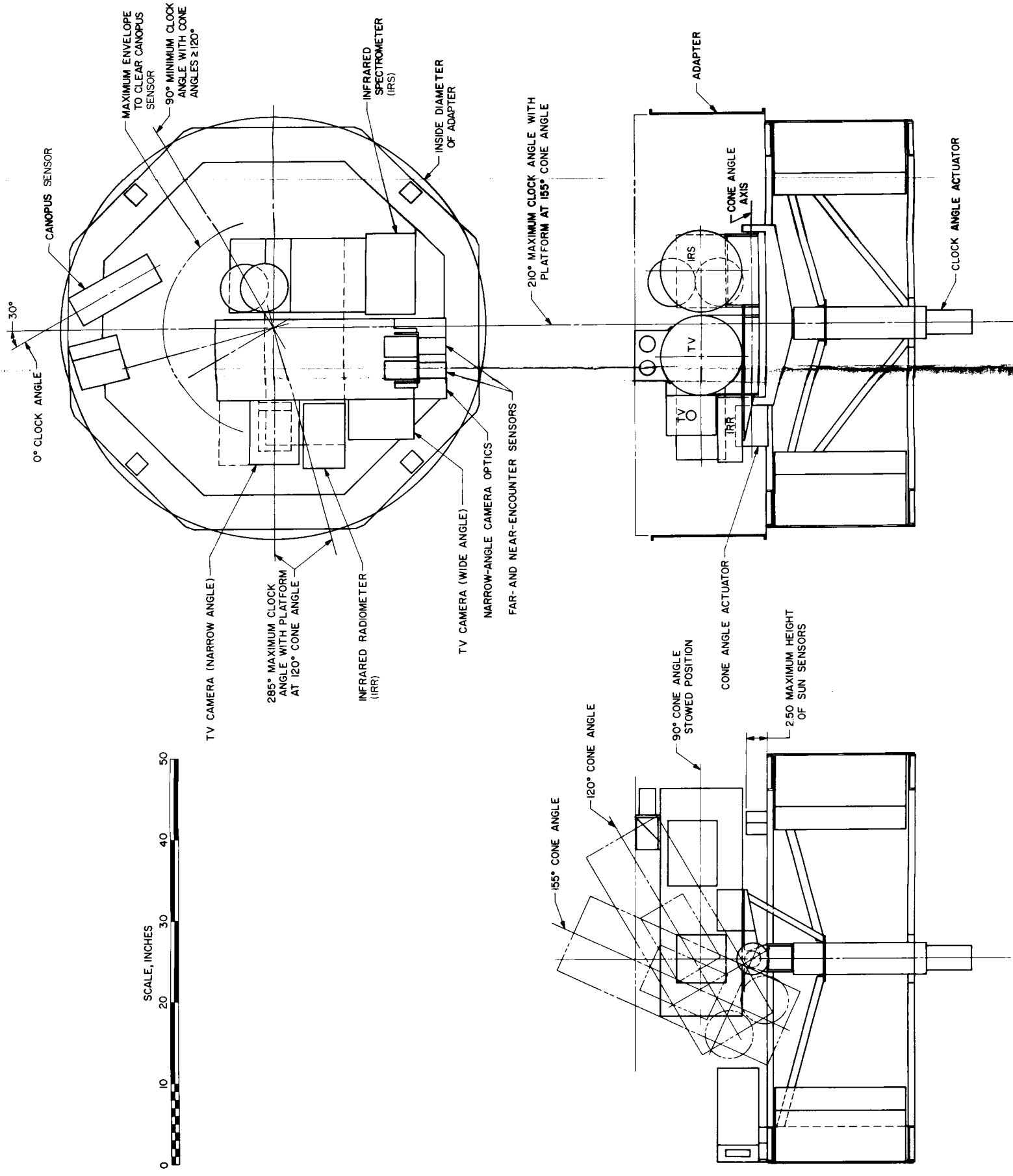**Fig. 1.** *Mariner Mars 1969 spacecraft configuration (contd)*

16-2

Table 1. *Mariner* Mars 1969 Scientific Investigators

Experiment	Scientific Investigator	Affiliation
TV	R. B. Leighton[a]	California Institute of Technology
	B. C. Murray	California Institute of Technology
	R. P. Sharp	California Institute of Technology
	N. H. Horowitz	California Institute of Technology
	J. D. Allen	Jet Propulsion Laboratory
	A. G. Herriman	Jet Propulsion Laboratory
	L. R. Malling	Jet Propulsion Laboratory
	R. K. Sloan	Jet Propulsion Laboratory
	N. Davies	Rand Corporation
	C. Leovy	Rand Corporation
Infrared spectrometer	G. C. Pimentel[a]	University of California, Berkeley
	K. C. Herr	University of California, Berkeley
Ultraviolet airglow spectrometer	C. A. Barth[a]	University of Colorado
	W. G. Fastie	Johns Hopkins University
Infrared radiometer	G. Neugebauer[a]	California Institute of Technology
	G. Munch	California Institute of Technology
	S. C. Chase	Santa Barbara Research Center
S-band occultation	A. J. Kliore[a]	Jet Propulsion Laboratory
	D. L. Cain	Jet Propulsion Laboratory
	G. S. Levy	Jet Propulsion Laboratory
Celestial mechanics	J. D. Anderson[a]	Jet Propulsion Laboratory

[a] Principal Scientific Investigator.

C. Spacecraft Mechanical Configuration

The *Mariner* Mars 1969 spacecraft configuration shown in Fig. 1 draws heavily on the *Mariner* Mars 1964 spacecraft design and the operational experience gained during that project. The principal changes are due to: (1) the use of the *Atlas/Centaur SLV-3C* launch vehicle, rather than the *Atlas D/Agena D* used for the *Mariner* Mars 1964 spacecraft; (2) the scientific payload requirements; and (3) the spacecraft trajectory during the pre-encounter and post-encounter periods. The *Mariner* Mars 1969 spacecraft, being about 40% heavier than its predecessor, can be considered as having four distinct segments:

1. Octagonal Electronics Compartment

This compartment, the basic structural foundation of the spacecraft, houses the electronics of the engineering subsystems, the major portion of the attitude-reference and -control elements, and the temperature-control subsystem. Seven of its eight bays contain electronics, and the eighth contains the propulsion subsystem. In contrast to the *Mariner* Mars 1964 propulsion subsystem which was mounted on the inboard side, the *Mariner* Mars 1969 propulsion subsystem may be mounted on the outboard edge of the octagon (in Bay 2) to provide volume internal to the octagon for structural support of the scan platform. All of the electronics bays are structurally integrated with the octagon such that the electronics assemblies carry a portion of the loads imposed on the octagon.

Two standard electronics assembly designs are utilized on the *Mariner* Mars 1969 spacecraft. For *Mariner* Mars 1964-type equipment, the electronics assembly configuration and geometry conform to the *Mariner* Mars 1964 design. A typical *Mariner* Mars 1964-type assembly is shown in Fig. 2. The second type of standard assembly configuration is shown in Fig. 3. The new design allows access to each subassembly from the spacecraft outboard side, but there is a limitation to the accessibility. Threaded fasteners are required between the assembly and subassemblies on the inboard side for dynamic stability and thermal control; however, it is anticipated that these fasteners will not be installed at the time when subassembly access is most often required. The assembly mounting hardware is also accessible from the outboard side of the spacecraft, thereby facilitating removal of an entire assembly. A rack and panel connector configuration allows the assembly harness to be hard-mounted, thus improving reliability. Another benefit is a lessening of the dynamic response of the subassemblies, since they

---

in the near future. Two fixed arrival dates will be utilized over the launch period for the two spacecraft. A minimum 1-month launch period is a project requirement for the *Mariner* Mars 1969 missions. To simplify encounter operations, the arrival dates will be separated by several days. The arrival dates tentatively selected, August 1 and 7, 1969, yield communications distances at encounter of 97 and 101 million km, respectively.

Two aiming points are also being considered for the two spacecraft. One is located so the scan traces of the TV and infrared spectrometer will pass approximately 5 deg below the northern edge of the south polar cap near closest approach. The other is located so that the scan traces will reach a maximum south latitude of approximately 30 deg. Both are such that: (1) the spacecraft will pass on the illuminated side of Mars at a nominal periapsis altitude of approximately 3000 km; and (2) the spacecraft will travel behind Mars as viewed from the Earth, resulting in Earth occultation.
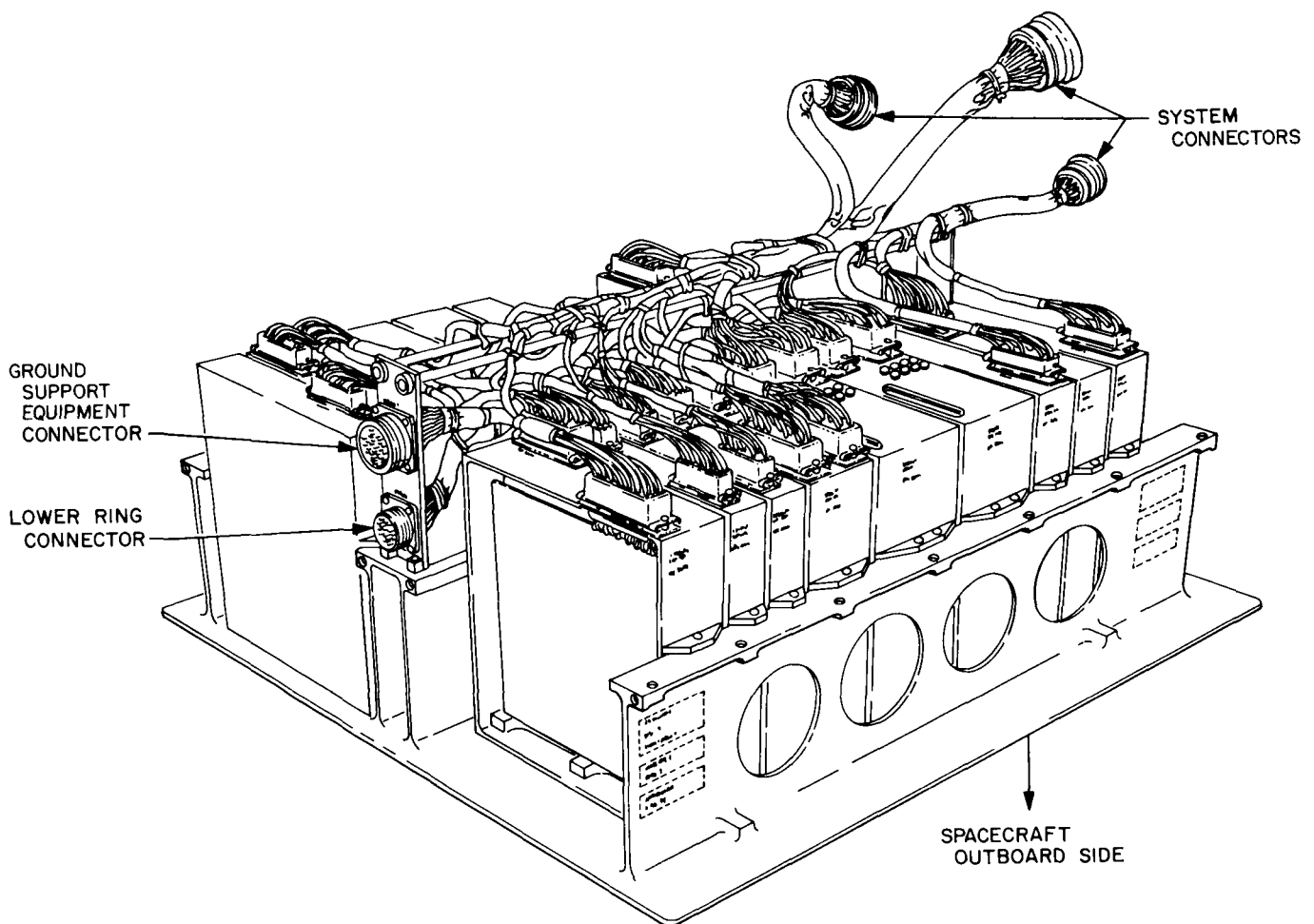
Fig. 2. Typical *Mariner* Mars 1964 electronics assembly

are fastened to shear panels on both the inboard and outboard sides.

Although the *Mariner* Mars 1964 packaging configuration has proved quite successful, it is felt that the new configuration will provide improved reliability and will facilitate spacecraft checkout. Testing and analysis of the new configuration is continuing.

2. Scan Platform

The scan platform provides mounting locations and subsystem support for the scientific experiments, as well as sensors and actuators to provide platform pointing. To achieve the pointing requirements of the scientific instruments, the scan platform has two degrees of freedom. The scientific experiments mounted on the scan platform are two TV cameras, the infrared radiom-

eter, the infrared spectrometer with a gaseous cooling system, and the ultraviolet spectrometer (not shown in Fig. 1). The total scientific instrument weight on the platform is in the 80- to 90-lb range. This weight, together with weight estimates for components such as the sensors, actuators, and structure, brings the total pointable mass to approximately 130 lb. The combination of the weight, volume, cabling, and scientific instrument view-angle requirements makes the *Mariner* Mars 1969 spacecraft scan platform significantly more complex than that of the *Mariner* Mars 1964 spacecraft. In fact, the most significant departure from the *Mariner* Mars 1964 spacecraft design is the complexity of the scan platform.

3. Forward Equipment Area

The forward equipment area includes the solar panels and spacecraft antennas. Current estimates of the solar
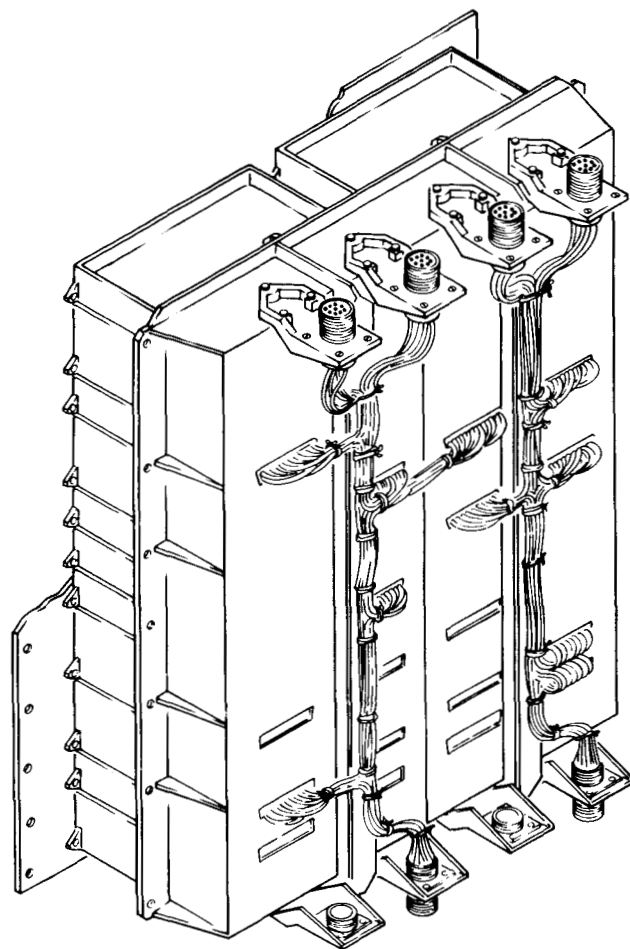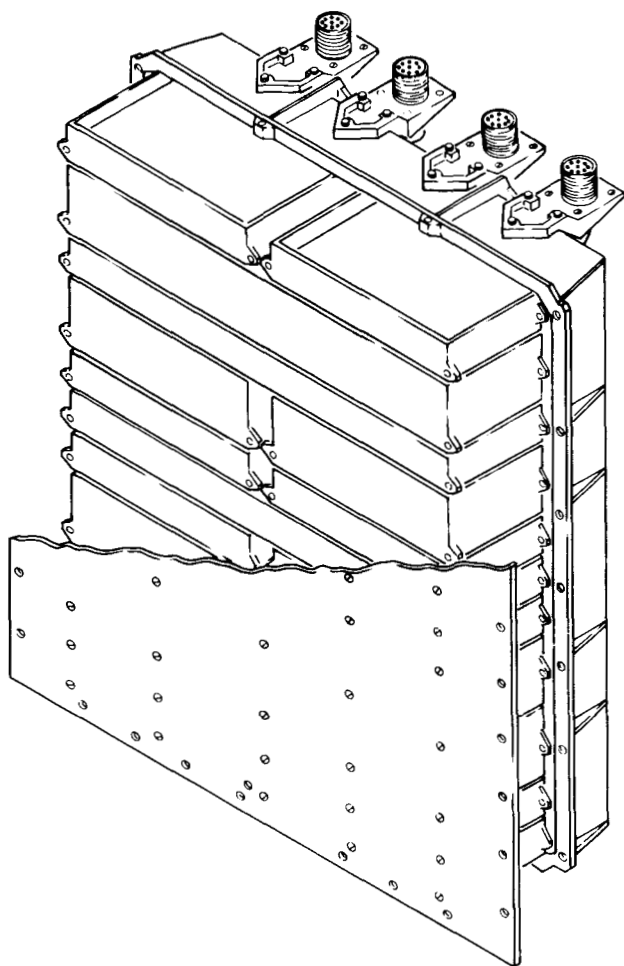
Fig. 3. Typical *Mariner* Mars 1969 electronics assembly

panel area requirement for the *Mariner* Mars 1969 spacecraft are in the 70- to 85-ft² range. Approaches to meeting this requirement vary from the use of four *Mariner* Mars 1964-type deployable panels, with small additional fixed panels, to the use of large-area deployable panels of a new design. All approaches will be evaluated as part of the total configuration design. The communications antennas to be used on the spacecraft are of the same design as those for the *Mariner* Mars 1964 spacecraft.

4. Adapter Section

The adapter section provides the primary interface and transition structure between the spacecraft and the launch vehicle, attachment and separation devices, and additional auxiliary equipment. The *Mariner* Mars 1969 spacecraft is shaped to fit within the envelope provided by the *Centaur* nose fairing, which is a cone approximately 120 in. in diameter and 190 in. long. The

spacecraft–nose fairing clearances allow for the dynamic environment of boost and for the clamshell separation of the nose fairing.

D. Design and Development

1. Temperature-Control Subsystem

For the *Mariner* Mars 1969 spacecraft, only hardware that is predominately for temperature-control purposes constitutes the temperature-control subsystem. Where possible, the spacecraft temperature-control requirements will be included in the thermal design of each part of the spacecraft.

At this time, it appears that the temperature-control hardware will consist primarily of louver assemblies and thermal shields. Certain specialized items may be included at a later time. The louver assemblies will be essentially the same as, and will be interchangeable with, those used on the *Mariner* Mars 1964 spacecraft. Two

minor changes are planned: (1) removal of the telemetry louver position indicator, and (2) addition of an optional provision for limiting the angle to which the louver is allowed to open. Due to changes in power distribution within the spacecraft and the geometry of the upper and lower surfaces of the bus, most of the detail design of the polished-aluminum bolt-on thermal shields will be changed. The over-all design of these and the multi-layered insulation blankets will, however, be similar to that of the *Mariner* Mars 1964 units.

A temperature-control flux monitor is also included as part of the temperature-control subsystem. It was developed to help resolve some of the difficulties previously experienced due to a lack of knowledge of the absolute value of the solar flux intercepted by the spacecraft. Errors of the order of 10 to 15% were experienced during the *Mariner IV* mission, resulting in temperature variations as much as 30°F from predictions. The flux monitor appears to be capable of measurements with an absolute error less than 1.5%. Laboratory models of the instrument have been fabricated and tested; these are presently being used as the primary reference radiometers during temperature-control testing in the JPL space simulators.

2. Spacecraft Mechanisms

The *Mariner* Mars 1969 spacecraft mechanisms will be similar in design to those of the *Mariner* Mars 1964 spacecraft wherever parallel functional requirements exist. Where device requirements are similar but sufficiently changed to require a new design, the *Mariner* Mars 1964 conceptual approach will be incorporated.

The designs of the low-gain-antenna, solar-panel-boost, and solar-panel-cruise dampers will be conceptually similar to the *Mariner* Mars 1964 designs; however, hardware details will be different, with a possible exception being those of the solar-panel-cruise dampers. The solar panel actuators and open switches, the pyrotechnic arming switch, and the separation-initiated timer are expected to remain unchanged, except for the addition of a thermal expansion compensator to the separation-initiated timer (a minor modification).

The major spacecraft mechanism redesign will be made on the planetary scan platform. The most severe platform resonances may have to be controlled during launch, in which case a scan platform resonance-control system will have to be designed and most likely incorporated into the scan platform latch system.

3. Gyro Control Assembly

The only changes which will be made to the gyro control assembly used on the *Mariner* Mars 1964 spacecraft will be those to increase the reliability of the system, rather than functional changes to improve its performance or efficiency. The changes proposed for the gyro electronics are minimal.

IV. Voyager Project

A. Introduction

1. Project Objectives

The primary objective of the *Voyager* Project is to carry out scientific investigations of the solar system by instrumented, unmanned spacecraft which will fly by, orbit, and/or land on the planets. Emphasis will be placed on the acquisition of scientific information relevant to the origin and evolution of the solar system and the origin, evolution, and nature of life; and the application of this information to an understanding of terrestrial life. The primary objective of the *Voyager* missions to Mars beginning in 1973 is to obtain information relative to the existence and nature of extraterrestrial life; the atmospheric, surface, and body characteristics of Mars; and the planetary environment by performing automated experiments on the surface of, and in orbit about, the planet. A secondary objective is to further our knowledge of the interplanetary medium between the planets Earth and Mars by obtaining scientific and engineering measurements while the spacecraft is in transit.

2. Project Plan

All *Voyager* missions will be conducted as events of an integrated program in which each individual flight forms a part of a logical sequence in an over-all technical plan of both lander and orbital operations. The *Voyager* de-

sign will provide for the transport of large scientific payloads to the planet, the telemetering of a large volume of data back to Earth, and long useful lifetimes in orbit about the planet and/or on the planetary surface. Hardware will be designed to accommodate a variety of spacecraft and/or capsule science payloads, mission profiles, and trajectories. Particular emphasis will be given to simple and conservative designs; redundancy wherever appropriate; and a comprehensive program of component, subsystem, and system testing.

Since no deep space flight tests of the flight spacecraft are planned, compensation will be made by additional ground tests conducted to the extent possible. During the test program for the flight capsule, which is planned to include Earth-entry flight tests, entry dynamics will be investigated.

Over-all direction and evaluation of the *Voyager* Project is the responsibility of the NASA Office of Space Science and Applications (OSSA). The project's management and the implementation of selected systems are the responsibilities of JPL.

3. Technical Description of Vehicles

Two *Voyager* planetary vehicles are to be designed, constructed, and tested for launch, using a single *Saturn V*

launch vehicle, during the 1973 Mars opportunity. Attention is also being given to requirements imposed on such vehicles by launches subsequent to 1973, such as a similar mission planned for 1975. Each planetary vehicle is to consist of a flight spacecraft and a flight capsule, with science experiments conducted both from the orbiter and on the planetary surface for the 1973 mission. The flight spacecraft, with several hundred pounds of science payload, will weigh approximately 2500 lb; its retropropulsion subsystem may, in addition, weigh up to 15,000 lb; and the flight capsule will weigh about 5000 lb. The flight spacecraft will be a fully attitude-stabilized device utilizing celestial references for the cruise phase. Velocity increments for midcourse trajectory corrections and for Mars orbit attainment by both the flight spacecraft and flight capsule will be provided. Onboard sequencing and logic and ground command capability will also be provided. The flight spacecraft will supply its own power from solar energy or from internal sources and will be capable of maintaining radio communications with Earth. In addition, the flight spacecraft will be thermally integrated and stabilized. Data concerning various scientific phenomena near Mars and during transit and those concerning spacecraft performance will be monitored and telemetered to Earth.

The flight spacecraft will also provide the flight capsule with services such as power, timing and sequencing, telemetry, and command during the transit portion of the missions and may also serve as a communications relay. The sterilized flight capsule will consist of a capsule bus and a surface laboratory system. The capsule bus will be designed for separation from the flight spacecraft in orbit; attainment of a Mars impact trajectory; entry into the Martian atmosphere; descent to the surface; and soft landing the surface laboratory, which will have a surface lifetime of up to 2 days in 1973. Later goals for surface lifetimes are as much as 6 mo. The capsule bus will contain the propulsion, power, guidance, control, communications, and data handling systems necessary to complete its mission, while the surface laboratory will contain all power, sequencing, and communications systems for the conduct of surface investigations.

B. Design and Development

1. Attitude-Control Triple-Redundant Circuits

Breadboard construction and testing of the attitude-control triple-redundant circuits proposed in the spacecraft conceptual design of December 1965 have been under way since that time. The basic electronics circuit for a single axis of control is made up of three distinct parts: (1) triple-redundant power switches, (2) level detectors (with minimum on-time), and (3) analog amplifiers. A breadboard model of an entire power switch for the roll-control axis has undergone more than 5000 hr of life testing under various simulated failure conditions and is performing perfectly. Three of the level-detector circuits have been constructed, tested, and used to drive the power switch section; testing to date indicates the circuits are functioning correctly. The analog-amplifier circuit, which drives the level detector section, has also been constructed and tested.

An entire single-axis subassembly of the triple-redundant electronics has been completed and is ready for demonstration. Approximately 2750 hr of life testing have been accumulated on the over-all system.

2. High-Impact Traveling-Wave-Tube (TWT) Amplifier

A program to develop a TWT capable of surviving 10,000-g 1-msec shocks and its associated RF output filter is under way. Four series of high-impact tests of TWT components have been conducted. Design, fabrication, and testing of three different electron guns were required to meet the 10,000-g test requirement. The data from the fourth series of tests are still being analyzed. It seems likely that the problems remaining will be minor enough to allow fabrication of a complete TWT with a reasonable level of confidence.

The RF filter is a six-section low-pass and band-reject unit. The breadboard unit was shocked at 13,000 g for 0.5 msec, and the filter's electrical characteristics remained within specification limits. An engineering model was then fabricated with larger-diameter tuning probes, since these components showed significant deformation during the earlier tests. This unit passed the shock tests with no significant deformation. The qualification unit has been fabricated and will undergo shock tests of the specification requirement of 1-msec duration in the near future.

3. Spacecraft 50-w TWT Amplifier

A 50-w TWT amplifier is being developed for spacecraft use. The single package will contain a TWT, a power supply, and an RF output filter. The entire amplifier is to take DC power from a 25- to 50-v bus and produce an S-band output of 50 w from an input RF drive of 200 mw. The amplifier is to operate through critical breakdown pressures; thus, it will be able to

operate during launch or during entry in a planetary lander.

The most difficult requirement of the development effort for the TWT—meeting the 33%-efficiency (over-all) specification—is to be met by optimizing a standard single depressed-collector TWT design. For the power supply, two types of supplies are being developed: (1) a more advanced concept than the separate regulator and converter used for the *Mariner* Mars 1964 TWT power supply, and (2) a conventional supply based on the *Mariner* Mars 1964 design. The more advanced concept uses a conventional low-power regulator and converter to provide filament, anode, and helix voltages, but uses a power bridge circuit to regulate and invert power for the collector supply in a single operation. Development of both supplies will be continued until sufficient data are available to enable a decision as to the most desirable concept. The four-section bandpass RF filter will pro-

vide enough rejection at the spacecraft up-link frequencies to prevent TWT noise from causing an increase in the effective spacecraft receiver noise figure. This filter will also attenuate the TWT harmonics sufficiently to prevent RF interference from this source.

The first TWT fabricated deviated significantly from design parameters; therefore, a second tube has been fabricated and will be tested. The advanced power supply breadboard unit did not perform as expected, so an alternate breadboard unit with more conventional circuitry has been fabricated; however, no performance data on the second unit are yet available. Manufacturer's data on the first RF output filter prototype show that the rejection is greater than required at all frequencies of interest. Insertion loss is 0.4 db, the maximum allowed by the specification. No attempt to finalize the amplifier packaging design will be made until the major component designs have been made more definite.

V. DSN Capabilities and Facilities

DEEP SPACE NETWORK

Established by the NASA Office of Tracking and Data Acquisition and under the system management and technical direction of JPL, the Deep Space Network (DSN) is responsible for two-way communications with unmanned spacecraft traveling from approximately 10,000 miles from the Earth to interplanetary distances. [Earth-orbiting scientific and communications satellites and the manned spacecraft of the *Gemini* and *Apollo* Projects are tracked by the Space Tracking and Data Acquisition Network (STADAN) and the Manned Space Flight Network (MSFN), respectively.] NASA space exploration projects supported, or to be supported, by the DSN include the following: (1) *Ranger, Surveyor, Mariner* Mars 1964, *Mariner IV, Mariner* Venus 67, *Mariner* Mars 1969, and *Voyager* Projects of JPL; (2) *Lunar Orbiter* Project of the Langley Research Center; (3) *Pioneer* Project of the Ames Research Center, and (4) *Apollo* Project of the Manned Spacecraft Center (as backup to MSFN).

Present DSN facilities permit simultaneous control of a newly launched spacecraft and a second spacecraft already in flight. In preparation for increased U.S. activities in space, a capability is being developed for simultaneous control of either two newly launched spacecraft plus two in flight, or four spacecraft in flight. Advanced communications techniques are being implemented to enable obtaining data from, and tracking spacecraft to, planets as far out in space as Jupiter. The main elements of the DSN are described below.

A. Deep Space Instrumentation Facility

The Deep Space Instrumentation Facility (DSIF) is composed of tracking and data acquisition stations around the world. The deep space stations (DSS's) of the DSIF and the deep space communication complexes (DSCC's) they comprise are as follows:

DSS	DSCC
Pioneer Echo Venus Mars	Goldstone
Woomera Tidbinbilla Booroomba[b]	Canberra
Johannesburg	
Robledo Cebreros[c] Rio Cofio[b]	Madrid[a]
Cape Kennedy (spacecraft monitoring)	
Ascension Island (spacecraft guidance and command)	

[a] Planned.
[b] Station not yet authorized.
[c] Station not yet operational.

These stations are situated such that three may be selected approximately 120 deg apart in longitude in order that a spacecraft in or near the ecliptic plane is always within the field of view of at least one of the selected ground antennas. JPL operates the U.S. stations and the Ascension Island DSS. The overseas stations are normally staffed and operated by government agencies of the respective countries, with the assistance of U.S. support personnel.

The Cape Kennedy DSS supports spacecraft final checkout prior to launch, verifies compatibility between the DSN and the flight spacecraft, measures spacecraft frequencies during countdown, and provides telemetry reception from liftoff to local horizon. The other stations obtain angular position, velocity (doppler), and distance (range) data for the spacecraft and provide command control to (uplink) and data reception from (downlink) the spacecraft. Large antennas, low-noise phase-lock receiving systems, and high-power transmitters are utilized. The 85-ft-diameter antennas have gains of 53 db at 2300 MHz, with a system temperature of 55°K, making possible significant data rates at distances as far as the planet Mars. To improve the data rate and distance capability, a 210-ft-diameter antenna was built at the Mars DSS, and two additional antennas of this size are planned for installation at overseas stations. In their present configuration, all stations except the Johannesburg DSS are full S-band stations. The Johannesburg DSS receiver has the capability for L- to S-band conversion.

It is the policy of the DSN to continuously conduct research and development of new components and systems and to engineer them into the network to maintain a state-of-the-art capability. Therefore, the Goldstone DSCC is also used for extensive investigation of space tracking and telecommunications techniques, establishment of DSIF/spacecraft compatibility, and development of new DSIF hardware and software. New DSIF equipment is installed and tested at the Goldstone DSCC before being accepted for system-wide integration into the DSIF. After acceptance for general use, the equipment is classed as Goldstone Duplicate Standard in order to standardize the design and operation of identical items throughout the system.

B. Ground Communication System

To enable communications between all elements of the DSN, the Ground Communication System (GCS) uses voice, teletype, and high-speed data circuits provided by the worldwide NASA Communications Network between each overseas deep space station, the Cape Kennedy DSS, and the Space Flight Operations Facility (SFOF, described below). The NASA Communications Network is a global network consisting of more than 100,000 route mi and 450,000 circuit mi interconnecting 89 stations, of which 34 are overseas in 18 foreign countries. Entirely operationally oriented, it is comprised of those circuits, terminals, and pieces of switching equipment interconnecting tracking and data acquisition stations with, for example, mission control, project control, and computing centers. Circuits used exclusively for administration purposes are not included.

Voice, teletype, high-speed data, and video circuits between the SFOF and the Goldstone DSCC are provided by a DSN microwave link.

C. Space Flight Operations Facility

During the support of a spacecraft, the entire DSN operation is controlled by the Space Flight Operations Facility (SFOF) at JPL. All spacecraft command, data processing, and data analysis can be accomplished within this facility. Operations control consoles, status and operations displays, computers, and data processing equipment are used for the analysis of spacecraft performance and space science experiments. Communications facilities are used to control space flight operations by generating trajectories and orbits and command and control data from tracking and telemetry data received from the DSIF in near-real time. The telemetry, tracking, command, and station performance data recorded by the DSIF are also reduced at the SFOF into engineering and scientific information for analysis and use by scientific experimenters and spacecraft engineers.

VI. DSIF Development and Operations

DEEP SPACE NETWORK

A. Flight Project Support

1. Surveyor Project

The *Surveyor I* (*Surveyor A*) mission was officially terminated in July, at which time the Pioneer DSS began preparations for the *Surveyor B* mission. In general, the *Surveyor* equipment and the S-band system remained unchanged. Except for equipment relocation in the .S-band control room to permit installation of multiple-mission support area equipment, only minor assembly modifications were performed. Inter-area compatibility tests were completed.

2. Mariner Mars 1964 Project

Residual activities of this project include periodic *Mariner IV* detection/recording operations and command activity. The spacecraft is presently being tracked for several hours during 1 day each month. During the last scheduled tracking period on August 5, 1966, two-way lockup was established using the 85-ft-diameter antenna and the 100-kw transmitter at the Venus DSS for transmitting and the 210-ft-diameter antenna of the Mars DSS for receiving. Commands were transmitted to the *Mariner IV* low-gain omnidirectional antenna, and the resultant spacecraft telemetry was recorded.

3. Lunar Orbiter Project

Lunar Orbiter I was launched from Cape Kennedy, Florida, on August 10, 1966. The first view period for the Echo DSS came the following day. During the early portion of the fourth view period for the Echo DSS on August 14, commands were transmitted for the first orbital engine deboost firing.

Successful reception and video photographic processing of the spacecraft picture readouts were accomplished for the original high-orbit and the final low-orbit picture-taking sequences. In addition, time synchronization correlations were performed between the Echo DSS, Robledo DSS, and Woomera DSS, using the Mark I ranging subsystem.

4. Pioneer Project

The Mars DSS assumed the prime tracking of *Pioneer VI* on June 29, with telemetry and command processing being accomplished at the Echo DSS by means of microwave transmission in a manner similar to that described below for the Echo and Pioneer DSS operations for *Pioneer VII*. Until August 6, the Echo DSS also provided a transmitter and command function for the

Mars DSS. Because of prime power difficulties with the diesel generators, the Mars DSS delayed testing the 20-kw transmitter installation on the 210-ft-diameter antenna until additional prime power was provided. Beginning August 7, the Mars DSS assumed command transmission to *Pioneer VI*, freeing the Echo DSS for the approaching *Lunar Orbiter I* spacecraft operations. Telemetry and command processing and prime magnetic tape recording continues to be performed at the Echo DSS.

Pioneer VII was launched on August 17. The overlap of the *Lunar Orbiter I* and *Pioneer VII* view periods was such that the Echo DSS could have tracked only a portion of either spacecraft's passes on any given day. The nature of the early passes of both spacecraft made it imperative that full view periods be observed. Therefore, the Pioneer DSS, acting as backup to the Echo DSS for *Pioneer VI*, was designated the prime station for the launch and early tracking of *Pioneer VII*.

A Type II orientation operation was implemented. From the *Pioneer* ground operational equipment located in the Echo DSS control building, commands were first entered and verified through the telemetry and command processing (TCP) subsystem computer and then stored in the command encoder awaiting transmit time. Actuation of the transmit function microwaved the command from the Echo DSS to the Pioneer DSS transmitter and from there to the spacecraft. The spacecraft's telemetry was received at the Pioneer DSS and microwaved to the Echo DSS, where it was processed through the ground-operational-equipment demodulator/synchronizer and into the TCP computer for teletype routing to the SFOF.

Two TCP computers, designated Alpha and Beta, were the basic units for the TCP subsystem. Included were the transfer racks allowing rapid interchange between *Lunar Orbiter I* and *Pioneer VII* mission functions, the NASCOM high-speed data line equipment, and associated teletype printers. Normal operation provided for *Lunar Orbiter I* data processing through the Alpha computer and *Pioneer VII* data processing through the Beta computer. In the event of a computer failure during overlap tracking, the spacecraft priority at that time determined the use of the operational computer. Transfer between the computers could be accomplished nominally within 5 min, resulting in minimal loss of data.

During the second pass of *Pioneer VII* over the Pioneer DSS on August 18, the spacecraft high-gain antenna was aligned with the Earth, using the Type II orientation operation. A daily tracking schedule was maintained through the end of this reporting period.

5. Apollo Project

The Pioneer DSS, Tidbinbilla DSS, and Robledo DSS of the DSN are scheduled to be backup stations for the *Apollo* spacecraft tracking, should a failure or serious degradation of performance occur at the co-located prime station of the Manned Space Flight Network. The DSN stations normally will participate in the *Apollo* missions and their simulations on a full-time basis from 2 wk before launch until the end of the mission and on a scheduled basis at other times. The backup stations will each have a dual capability to permit simultaneous communications with two *Apollo* spacecraft. DSN equipment modifications required for support of the *Apollo* missions are presently being accomplished.

B. DSS Equipment Installation

1. Pioneer DSS

Requirements to maintain support of the normal DSN missions and also help in the implementation of the Manned Space Flight Facility (MSFF) required extensive changes at the Pioneer DSS. Installation of the S-band system for the MSFF began in July. The installation in the control room is shown in Fig. 1. Installed to date are the receiver and transmitter exciter, antenna servo electronics, antenna position programmer, tracking data processor, and portions of the telemetry equipment. Subsystem power-on tests, preliminary interfacing, and basic operational tests are in progress.

The additional weight of the second transmitter and the maser assembly requirements of the MSFF on the antenna required the addition of 4900 lb of counterweights to the hour-angle gear. Equipment relocations, new cable trays, and other changes to the declination room and antenna were also made. A cable wrapup, patterned after that developed for the Echo DSS 85-ft-diameter antenna, was installed and tested.

2. Echo DSS

The second analog instrumentation subsystem was delivered just prior to the final testing and launch of *Lunar Orbiter I*. The equipment racks were readied for interrack and interface cabling. Two magnetic tape recorders for the subsystem were installed and used for *Pioneer VI* and *VII* spacecraft recordings.

Fig. 1. MSFF control room installation at Pioneer DSS

To improve the interface of rate feedback signals with the MSFN servo electronics and to upgrade the rate loops of the standard DSIF 85-ft-diameter polar tracking antennas, it was decided to replace the present 400-Hz AC tachometers with DC tachometers. The testing and trial installation of the DC tachometer chosen (a standard DC permanent-magnet tachometer generator with built-in temperature compensation and a nominal gain of 20.8 v at 1000 rev/min) was performed on the Echo DSS antenna declination drive. The DC tachometer modification will be incorporated on all DSIF 85-ft-diameter antennas.

3. Venus DSS

The installation of all Venus DSS receiving subsystems was completed during this reporting period. After system checkout, the new central frequency synthesizer was turned over to the Venus DSS for operational use.

4. Mars DSS

The installation of the S-band system continues concurrently with Mars DSS operation. The 20-kw transmitter was placed in operation in August. The high-voltage

power supply for the transmitter (Fig. 2) is presently located in the large service area on the first floor of the pedestal. It will eventually be moved to its permanent position in the main equipment room on the alidade.

The 2388-MHz bistatic radar receiver consists of the following subsystems: (1) the Mars DSS 2388- to 30-MHz converter, (2) the Mars DSS 30-MHz to 455-kHz converter, (3) the Mars DSS 2388-MHz test transmitter, (4) the Mars DSS programmed oscillator, (5) the microwave link from the Mars DSS to the Venus DSS, (6) a portion of the Venus DSS Mod IV receiver, and (7) the Venus DSS correlator. The construction and installation of this receiver was completed during this reporting period, and the receiver was used for the Mercury bistatic planetary radar experiment discussed later in this section.

C. Communications Development and Testing

1. Evaluation of Traveling-Wave-Tube (TWT) Stability Characteristics

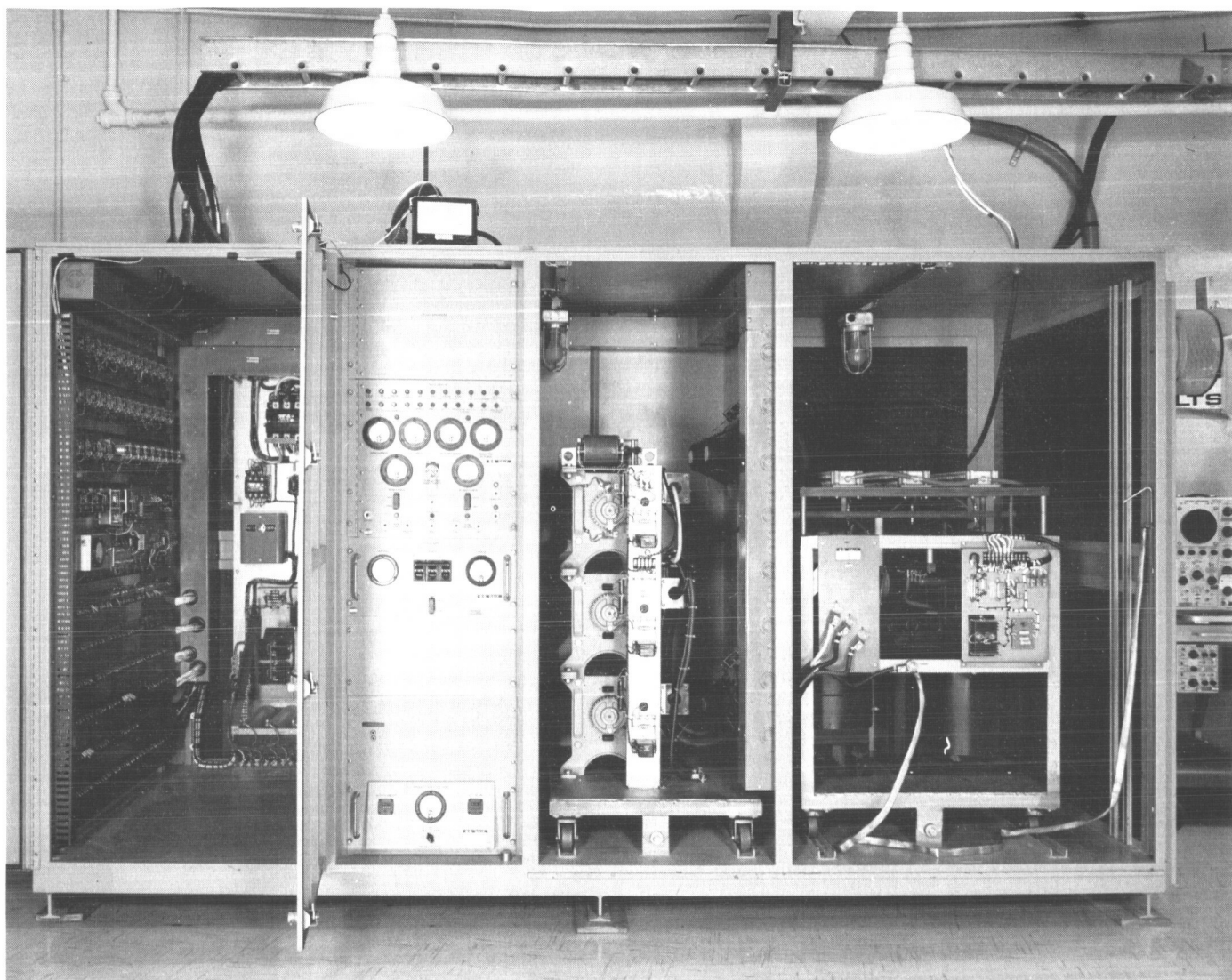A simple technique was used to evaluate the stability characteristics of a TWT. In addition to providing

Fig. 2. Mars DSS transmitter high-voltage power supply

pertinent information regarding the TWT as a possible follow-up amplifier to the atomic hydrogen maser, the experiment itself was important in establishing a technique for future evaluation of the atomic frequency standard.

This technique employs a phase bridge to measure the relative phase shift between two signal paths with the test device (unknown) in one of the paths. Two matched diodes are used as synchronous detectors and provide adequate sensitivity. To minimize differential phase errors due to frequency excursions in the signal generator, the electrical lengths of the two paths must be equalized by means of a precision S-band delay line in one of the paths. The calibrated delay line also provides

the means for calibrating the sensitivity of the phase bridge.

A calibration test was made with passive elements (coaxial cable) in both paths of the phase bridge. Short-term jitter was of the order of ±0.05 deg, and the drift over a 1-hr period was of the same order of magnitude. During the stability test with the TWT, the short- and long-term phase variation increased slightly to about ±0.25 deg. The regularity of the short-term jitter suggests the possibility of inadequate filtering in the built-in power supply. The cause of this jitter will be investigated.

The dual-channel traveling wave maser for the hydrogen line frequency (1420 MHz) is being completed. To

evaluate the short-term stability of the maser before it is used, stability tests such as those described here will be performed.

2. 85-ft Antenna/Research and Development (R&D) Cone System Noise Temperature Measurements

After installation of the R&D cone on the Venus DSS 85-ft-diameter antenna, two sets of preliminary noise temperature measurements of the system at 2388 Mc were made. These gave a value of approximately 22.0°K (with 0.4°K for the follow-up receiver), as compared to the 19.4°K system temperature measured for the R&D cone on the ground (assuming the same follow-up contribution for an equal-basis comparison).

This difference in system temperatures should be due to the difference in antenna temperatures. Therefore, when the system temperature difference of 2.6°K was added to the antenna temperature of 5.0°K measured for the R&D cone on the ground, the antenna temperature measured for the R&D cone on the 85-ft-diameter antenna should have been 7.6°K. However, examination of the preliminary data revealed that this temperature was approximately 6.6°K. The discrepancy of 1°K was believed to result from uncertainties in the liquid-nitrogen-cooled load used in the measurement. Further examination of the data showed that the receiver temperatures measured were greater than those measured when the cone was on the ground. A difference between the calibrated and actual value for the cryogenic load temperature can result in the measured receiver temperature being too high and the antenna temperature being too low.

A study is being made to determine the causes of discrepancies in the cryogenic load temperature. One possible source of error being investigated is the pressure differential between the atmosphere and the gas of the cryogenic fluid inside the dewar.

3. Evaluation of Beam-Shaping Flanges on Cassegrain Antenna Subreflectors

The subreflectors for the 85- and 210-ft-diameter antennas have flanges designed for S-band operation, since it has been found that these flanges can appreciably improve antenna efficiency. To evaluate the performance of these subreflectors at several frequencies, the subreflector configurations and illuminations were input to a JPL-developed computer program which calculates scattering from an arbitrary surface of revolution. The computed scattered patterns were then input to another computer program which evaluates antenna efficiency. Both subreflectors were evaluated at S-, C-, X-, and K_u-band. The resulting computed scattered patterns showed that operating above the design frequency causes substantial distortion at the edges of the patterns. The phase patterns are also perturbed in this region. It was concluded that the flange results in substantial improvement in performance at the design frequency and has very little effect on efficiency, either positively or negatively, at the higher frequencies.

An interesting result of the evaluation was that the flange was found to be much more effective on the smaller subreflector. The illumination efficiency of the smaller antenna is actually greater than that of the larger antenna —a complete reversal of the normal situation as illustrated by the no-flange case. This is caused by the fact that, on the smaller subreflector, the flange subtends a larger portion of the feed pattern, resulting in 3% less forward spillover. This more than makes up for the larger diffraction effects of the smaller subreflector. However, making the flange and/or the hyperboloid larger for the larger subreflector would result in undesirable effects. Therefore, it appears that, for the hyperboloid/flange combination, small subreflectors are better than large subreflectors. The difference in efficiency is small, but it indicates an area of potential improvement in the design of large subreflectors.

4. S-Band Cassegrain Monopulse (SCM) Cone Assembly Tests

As part of a continuing effort to maintain a state-of-the-art capability in the microwave antenna subsystem of the DSIF, advanced development has begun on the design of waveguide components capable of handling from 500- to 2000-kw continuous-wave transmitter power. During this reporting period, testing of present Goldstone Duplicate Standard components to determine their limitations under very high power was extended with the testing of a complete SCM cone assembly at power levels up to 100 kw continuous-wave. These tests were performed at the Venus DSS, using an available 100-kw klystron. An anomalous result of the tests which is being further investigated was peculiar behavior of the system noise temperature during diplexing at high power levels. Despite difficulties with harmonic power, the 100-kw SCM cone assembly tests were highly successful and indicate that the design goal of 2000-kw continuous-wave microwave components may well be achieved in the relatively near future.

5. Step-Recovery-Diode Multiplier Development

A ×8 frequency multiplier has been developed for use in the planned modification of the DSIF tracking system local oscillator and transmitter exciter multiplier chains. The existing multiplier chains in the system include a ×32 module. In the modified chain, this multiplication is accomplished by two units: a solid-state ×4 and amplifier module and the step-recovery-diode ×8 unit. Use of a step recovery diode makes possible efficient high-order frequency multiplication without the attendant circuit complexities of Varactor frequency multipliers.

A multiplication factor of 8 was chosen to achieve the power output required consistent with the input power capability of presently available diodes. This also places the input frequency in the very-high-frequency region of 260 to 280 Mc, where sufficiently high levels of power can be generated with transistor circuits. An added advantage of the ×8 unit is that the nearest sideband at the output is 260 to 280 Mc away from the center of the output bandpass. This allows sufficient suppression of undesired sidebands to tolerable levels with a minimum number of output filtering stages. The design was made as simple as possible without compromising performance so that the unit would be easily reproducible and require a minimum amount of testing.

The step recovery diode is mounted in a two-cavity output bandpass filter and is series-fed through a low-pass filter which isolates the input network from the output network. The diode taps directly into the center conductor of the first output filter cavity. The two output cavities are coupled through an iris in the common wall between them. Output coupling is accomplished with a loop. The tuning range of the multiplier was made sufficiently wide to allow use of the same unit for both exciter and local oscillator applications by applying the appropriate input signal and tuning the output cavities to the corresponding output signal. The tuning of the output cavities is accomplished by varying the length of the center conductors. The same basic unit was also operated as a ×16 multiplier by redesigning the low-pass filter for a lower cutoff frequency, and performance was quite satisfactory.

6. 1-mw High-Voltage Power Supply Testing

Tests were performed on the 1-mw power supply at the Venus DSS to substantiate the conclusion reached during previous tests that the high-voltage ripple and noise could be reduced by replacing the amplidyne exciting the field of the 400-Hz generator with a faster-responding programmable solid-state power supply. A breadboard model of a simple 400-Hz, 3-phase, full-wave bridge silicon-controlled-rectifier power supply replaced the amplidyne, and a solid-state differential amplifier replaced the vacuum-tube regulator amplifier normally used in the system. The tests fully demonstrated that the beam voltage's low-frequency ripple characteristics can be significantly improved by such replacements.

Because of these and previous results, a specification was written for a programmable 175-v, 100-amp, solid-state power supply. Two units are currently being fabricated: one to excite the 1200-kw, 400-Hz generator, and the other to excite the 1750-hp drive motor.

7. Mercury Bistatic Planetary Radar Experiment at the Venus DSS

From July 12 to August 5, a bistatic planetary radar experiment with Mercury as the target was conducted at the Venus DSS. The transmitting antenna was the Venus DSS 85-ft-diameter azimuth-elevation antenna, and the receiving antenna was the Mars 210-ft-diameter azimuth-elevation antenna. The signal was fed to the Venus DSS at 455 kHz by means of the intersite microwave link, with both ranging and total spectrum data being collected. At the end of the experiment, the actual round-trip range was less than the predicted value by approximately 2350 μsec, or approximately 438 mi.

VII. Space Instruments

SPACE SCIENCES

A. Mars Cartography From the *Mariner IV* TV Pictures

To determine the nominal locations of the 22 TV pictures of Mars taken by *Mariner IV*, information concerning the approach trajectory was combined in a computer program with information on the relative pointing direction of the TV camera, as well as the ephemerides for planet orbit position and axial rotation. This TV constraints program had been successfully used to compute the *Ranger* TV picture coverage of the Moon. The estimated locations were then mapped on the best available charts of Mars depicting the regions that had been photographed. One of the resulting maps is presented in Fig. 1.

If the ephemeris-derived latitude and longitude coordinate grids of Mars are to be considered as an absolute reference system, then the following four significant error sources affect the estimates of picture locations:

(1) Spacecraft trajectory uncertainties.

(2) Mars radius uncertainty.

(3) Camera misalignment with respect to the nominal Sun and Canopus sensor pointing directions measured from the spacecraft.

(4) Spacecraft attitude uncertainty within the control limit cycles.

The accuracies of the encounter trajectory and camera alignment have been well-documented. An improved value for the Mars radius is not expected in the immediate future. Therefore, the attitude uncertainty remains as a major error source, since attitude-control data were not sent back during the TV picture-taking and -recording sequence (Data Mode 3).

Map location uncertainties relative to the nominal values were estimated with the help of the *Ranger* constraints program and the *Mariner* camera/Mars trajectory (MARCAM) program. The one-sigma uncertainty values were determined from the RMS contributions of the various error sources listed above. From these computations, the Picture 11 center location may be considered correct within 2 deg in latitude and 2.5 deg in longitude. For other pictures near the ends of the picture-taking sequence, the uncertainties are larger.

At first, it was assumed that spacecraft attitude at the time each picture was taken could be determined by backward extrapolation of telemetered data received within 15 min after Mars encounter. However, the irregularities in the data curves are evident in Fig. 2. It is seen that the acceleration during the first pitch loop was approximately 30% lower than that during the remaining loops. In the yaw and roll channels, few data points were available, since it was common for the roll and yaw jets to fire twice, rather than once, at the attitude limits.
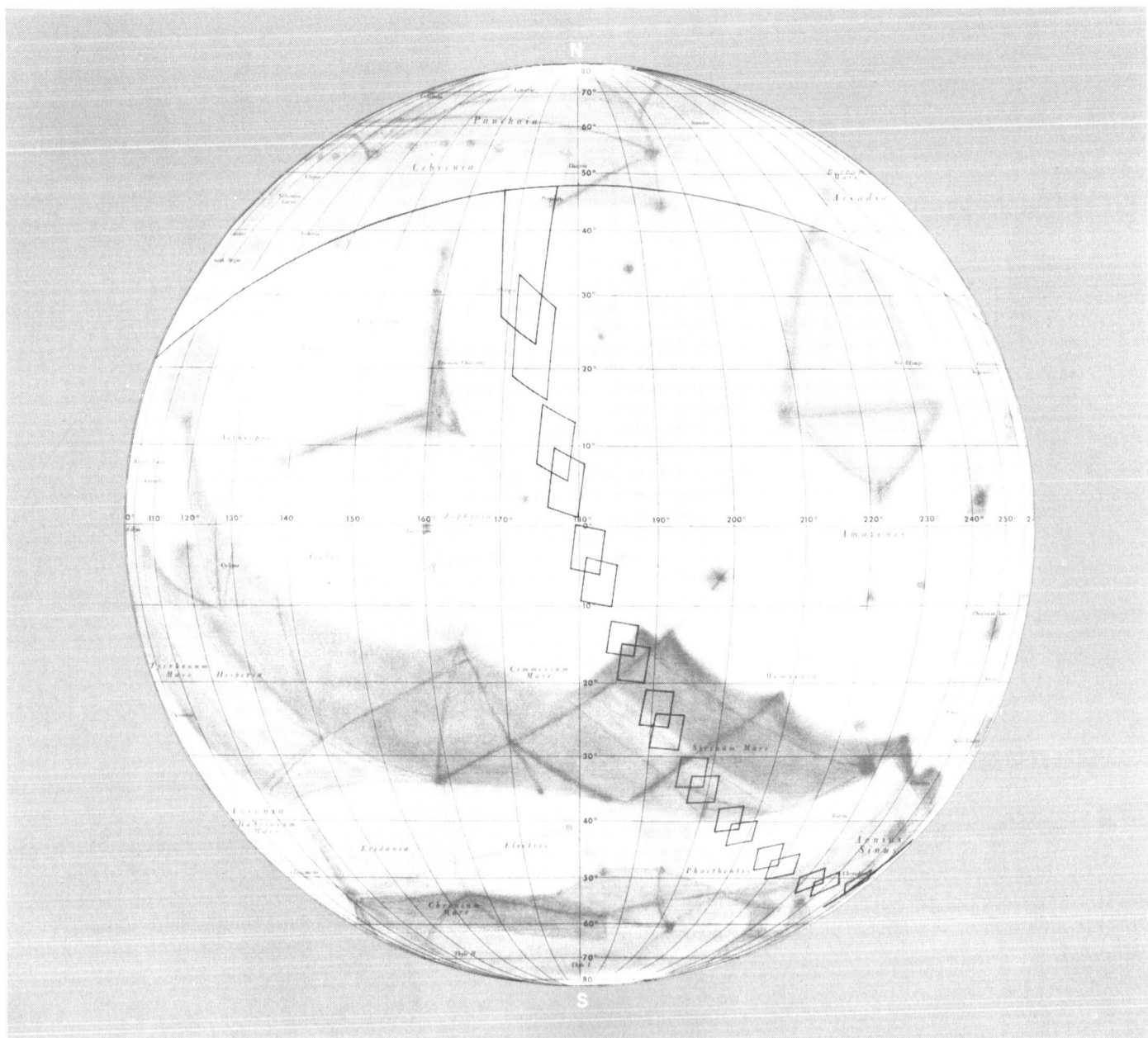
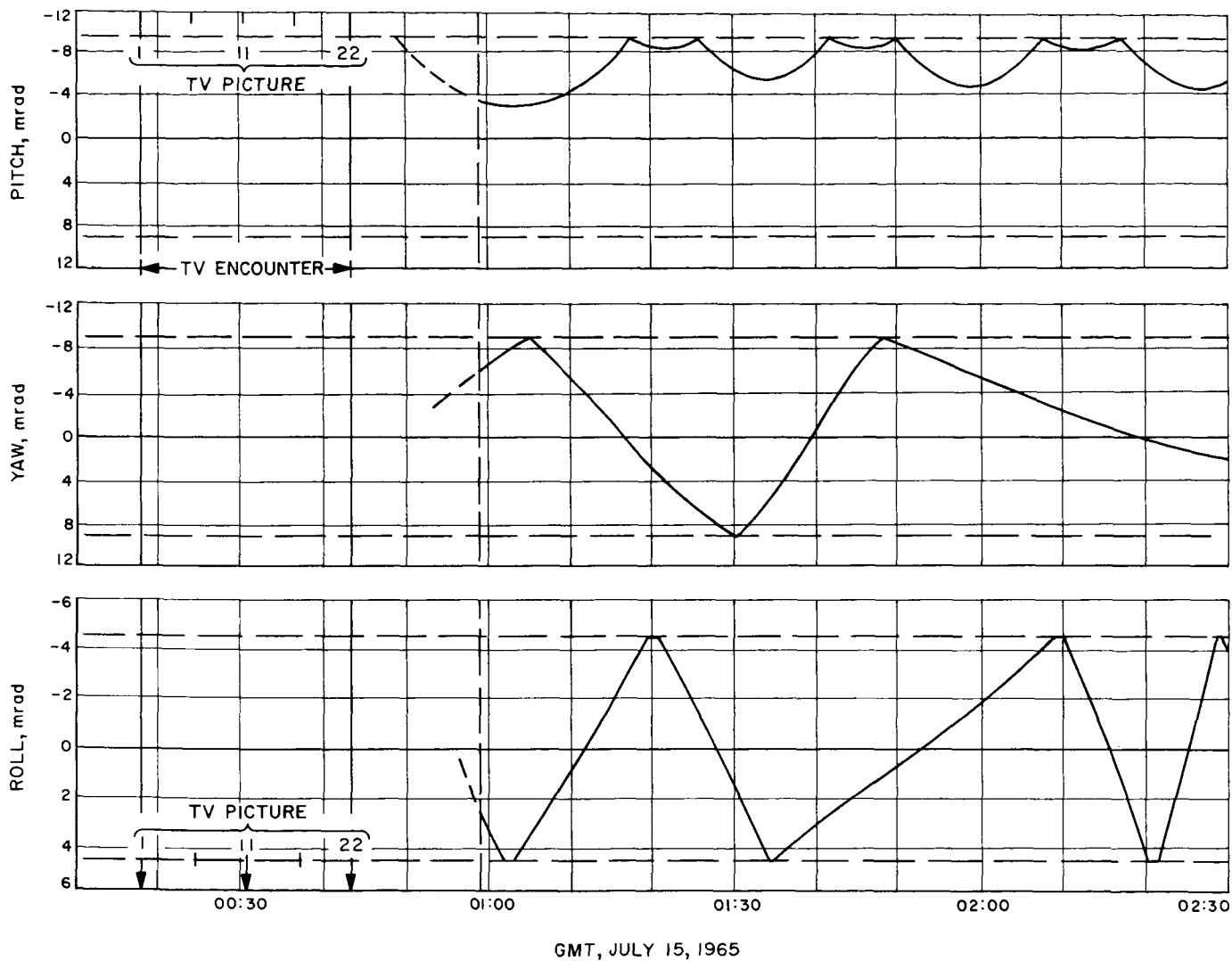Fig. 1. Map of Mars, showing nominal locations of *Mariner IV* TV pictures

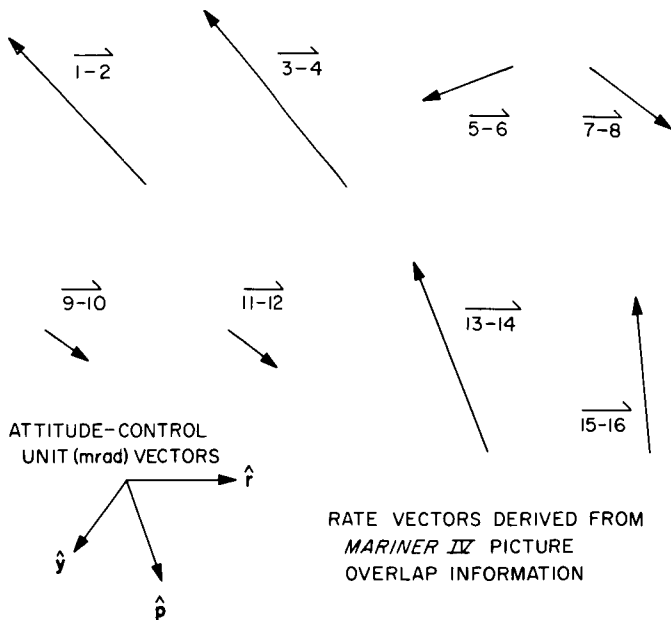Fig. 2. Mariner IV post-encounter attitude-control data

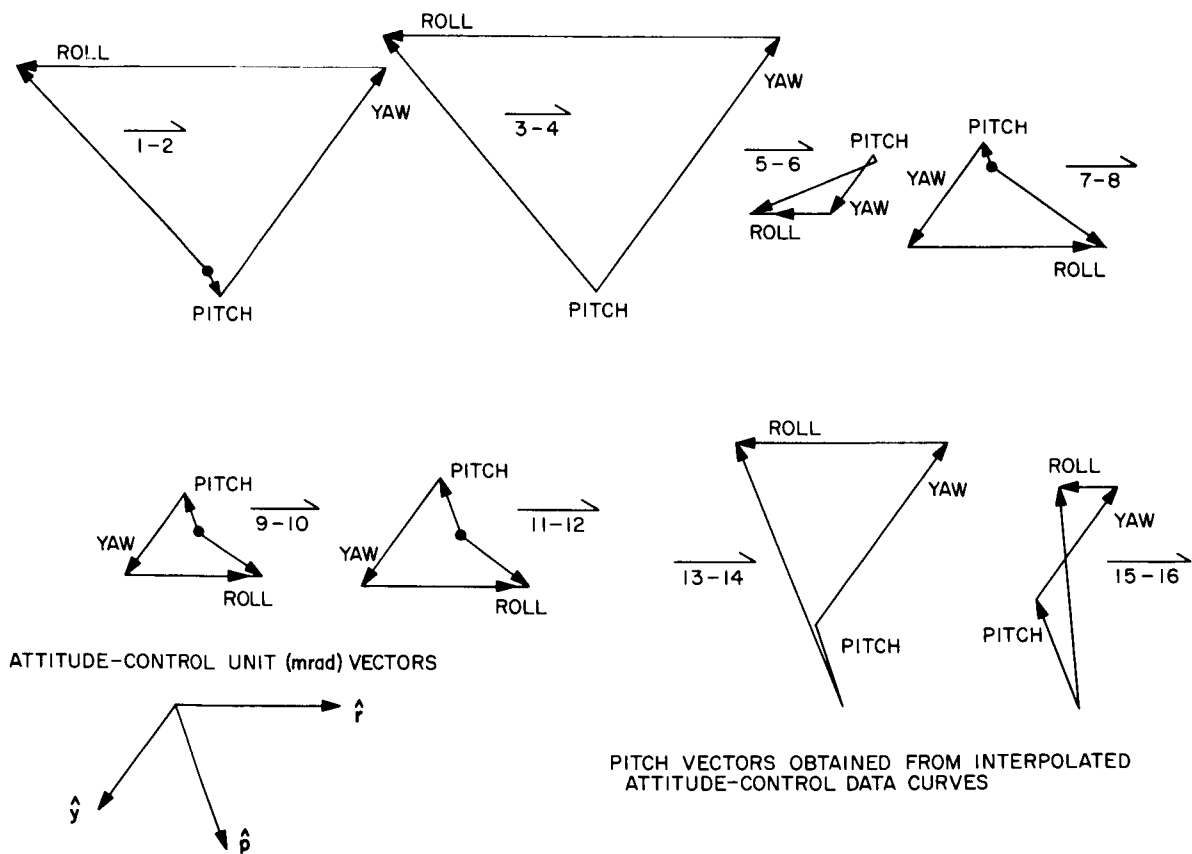Fig. 3. Rotation rate vectors between overlapping TV pictures

ATTITUDE-CONTROL UNIT (mrad) VECTORS

RATE VECTORS DERIVED FROM *MARINER IV* PICTURE OVERLAP INFORMATION

ATTITUDE-CONTROL UNIT (mrad) VECTORS

PITCH VECTORS OBTAINED FROM INTERPOLATED ATTITUDE-CONTROL DATA CURVES

Fig. 4. Resolution of rotation vectors

One checkpoint was available: the planet limb shown in Picture 1. Deceptively, it seemed reasonable that extrapolations could be based on the mean values of the measured leakage accelerations (from the shapes of the curves) and also on the rate increments measured at the turnaround points. When the most-probable extrapolated pitch, yaw, and roll values were input into the computer program, however, the planet limb came out in the wrong location.

Next, the picture overlap regions were examined to see in what direction the spacecraft was rotating during the interval between overlapping exposures. The resultant vectors (Fig. 3) indicate the amount of change in

position during the time between exposures and can serve as measures of rotation rates. For comparison, the position changes are also shown which would have resulted from a spacecraft rotation of 1 mrad in pitch, yaw, and roll during the same time interval. It appeared feasible to resolve the rotation vectors in terms of the respective unit vectors, and then these rates might be used to carry out the position extrapolations which had been attempted earlier. Since there were three unit vectors, however, it was not immediately possible to obtain unique solutions for the rate vectors.

At this point, the pre-encounter attitude-control data, which had ended approximately 2.5 hr before encounter,
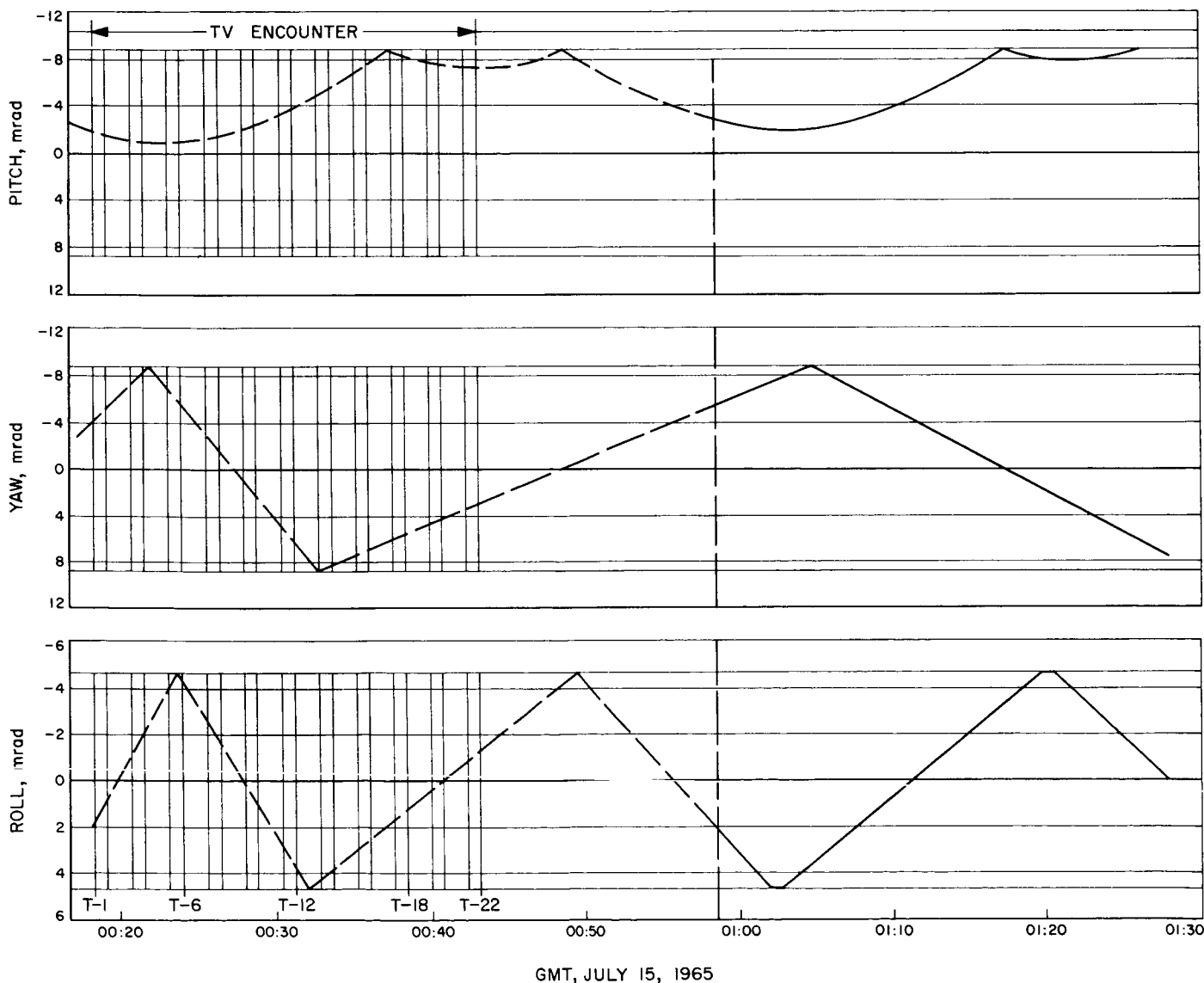

Fig. 5. Attitude-control data extrapolated through the TV picture-taking period

were also examined. It was found that the pitch-loop pairs (i.e., the large plus small loops) prior to encounter had periods of 40 ±2 min. When these data were extended forward through the time of encounter by adding approximately 3.5 of these 40-min loop pairs, it was found that the last loop merged with the first post-encounter pitch loop. This successfully defined the behavior of one of the three channels, making it possible to resolve the rotation vectors in terms of the other two unit vectors. The results are shown in Fig. 4. Some significantly large changes are obvious: (1) the yaw component changed from negative to positive between Pictures 4 and 5; (2) the roll rate changed from negative to positive

between Pictures 4 and 7 (apparently between 5 and 6); and (3) both the yaw and roll rates went from positive to negative between Pictures 12 and 13.

The hypothetical behavior of the limit cycles was used to supply the attitude-control data that had not been telemetered during encounter (Fig. 5). With this scheme, the planet limb in Picture 1 is placed in nearly the correct position. It now appears that the locations of many of the other pictures may be determined to better than 2-deg one-sigma uncertainty, corresponding to 120-km distance or approximately one-half the frame size.

VIII. Environmental Test Equipment

SUPPORTING ACTIVITIES

A. Contamination Collection Plate

During thermal-vacuum testing of developmental and flight spacecraft and components, certain materials may outgas and contaminate the interior of the vacuum chamber by causing miscellaneous material to be deposited on the cold shroud surrounding the test specimen. The subsequent decontamination of the chamber can be expensive and time-consuming.

A method has been developed by which contamination of the JPL Environmental Testing Laboratory 7- × 14-ft vacuum chamber itself can essentially be avoided:

(1) Maintaining the maximum test vacuum, a 2- × 2-ft stainless-steel plate mounted on the chamber door (Figs. 1 and 2) is cooled to cryogenic temperature (−300°F) with LN_2. (Quick disconnect lines for the LN_2 are available at a separate control and LN_2 manifold.)

(2) The shroud temperature is increased to ambient, and the chamber pressure is increased to approximately 400 torr.

(3) The plate temperature is then increased to ambient, and the chamber pressure is increased to atmospheric level.

(4) After the chamber door is opened, the plate with its accumulated contamination is cleaned with the appropriate solvent (e.g., acetone).

Thus, the chamber may be cleaned by washing *only* the contaminated plate. No other part of the chamber requires cleaning, since chemical analysis of the chamber shroud has shown little contamination after the above routine was followed. Extensive contamination was found on the plate during this analysis. The collected contaminants will not outgas again and thereby contaminate a spacecraft under test.

Since only the plate requires cleaning, cleanup time has been reduced from as much as 3 days to a few hours. The result is an increase in chamber availability and a decrease in operating costs. An added advantage is that, since the outgassed materials are collected on the plate, these materials can be easily identified, even though their quantity may be small.
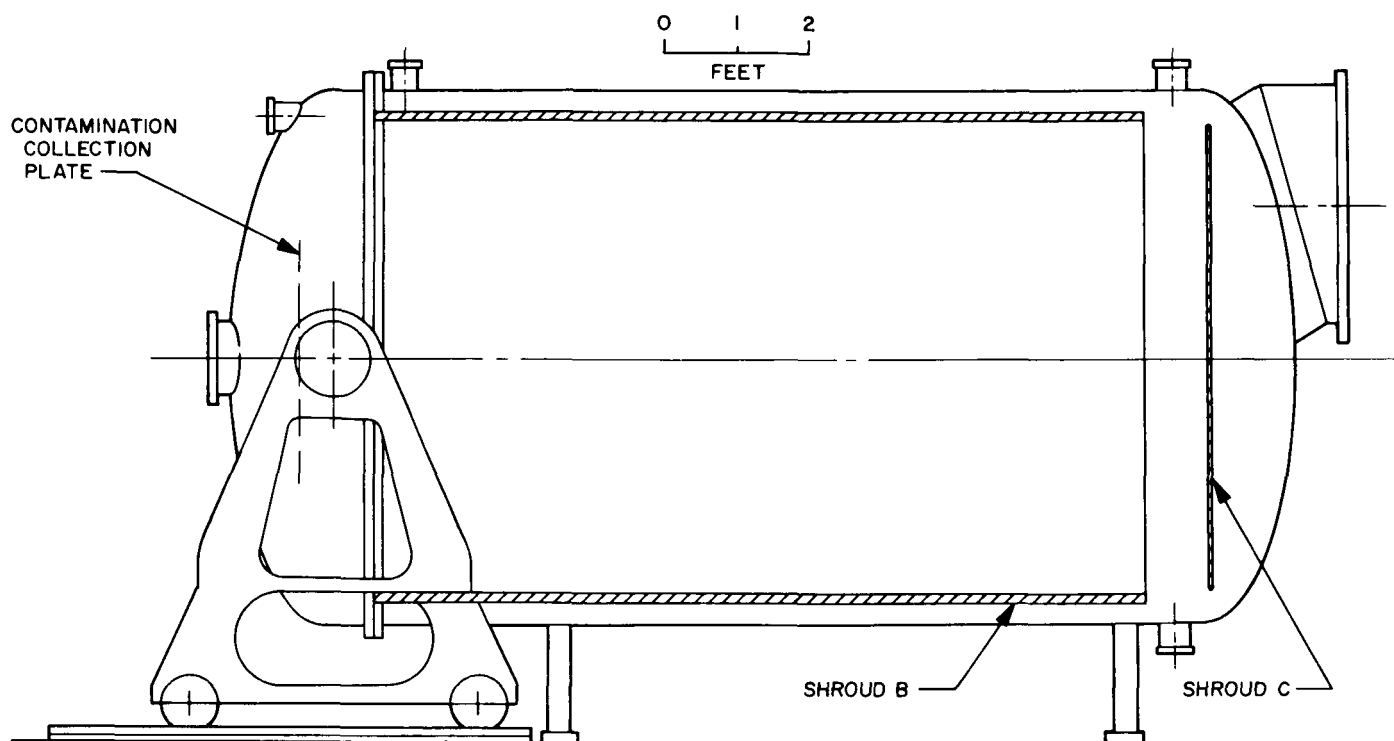
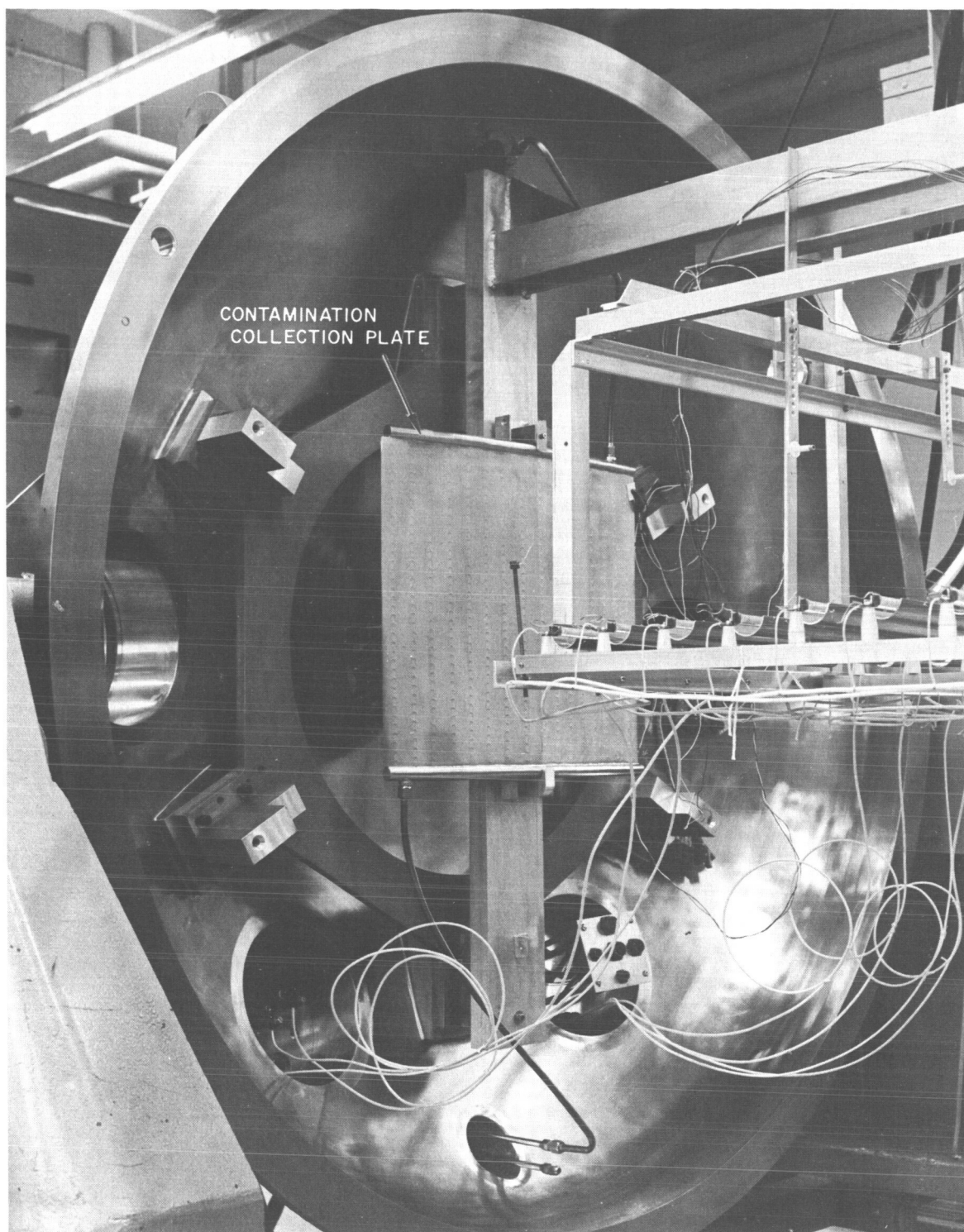Fig. 1. 7- × 14-ft vacuum chamber, showing location of contamination collection plate

CONTAMINATION
COLLECTION PLATE

Fig. 2. Contamination collection plate mounted on vacuum chamber door

B. Thermal Radiation Lamp Bank Reflector

Standard quartz infrared lamps have proven to be a satisfactory thermal source. However, the radiation pattern is circular along the tube axis, which causes a dispersion of radiating energy and a loss of radiation to the space chamber wall.

A light-weight quartz-lamp reflector has been developed which provides a simple and inexpensive means of increasing the radiation intensity and uniformity in the test plane. This reflector, shown in Fig. 3, will be used for thermal-vacuum radiation simulation on *Mariner* Venus 67 and *Surveyor* spacecraft solar panels. The self-supporting reflector is made of thin aluminum tubing which is split in half and highly polished on the inside. The reflector is mounted on the lamp by two wire clips, as may be seen in Fig. 3. Adjustment of the lamp ends and directional adjustment of the reflector provide a means for regulating thermal properties at the test plane.
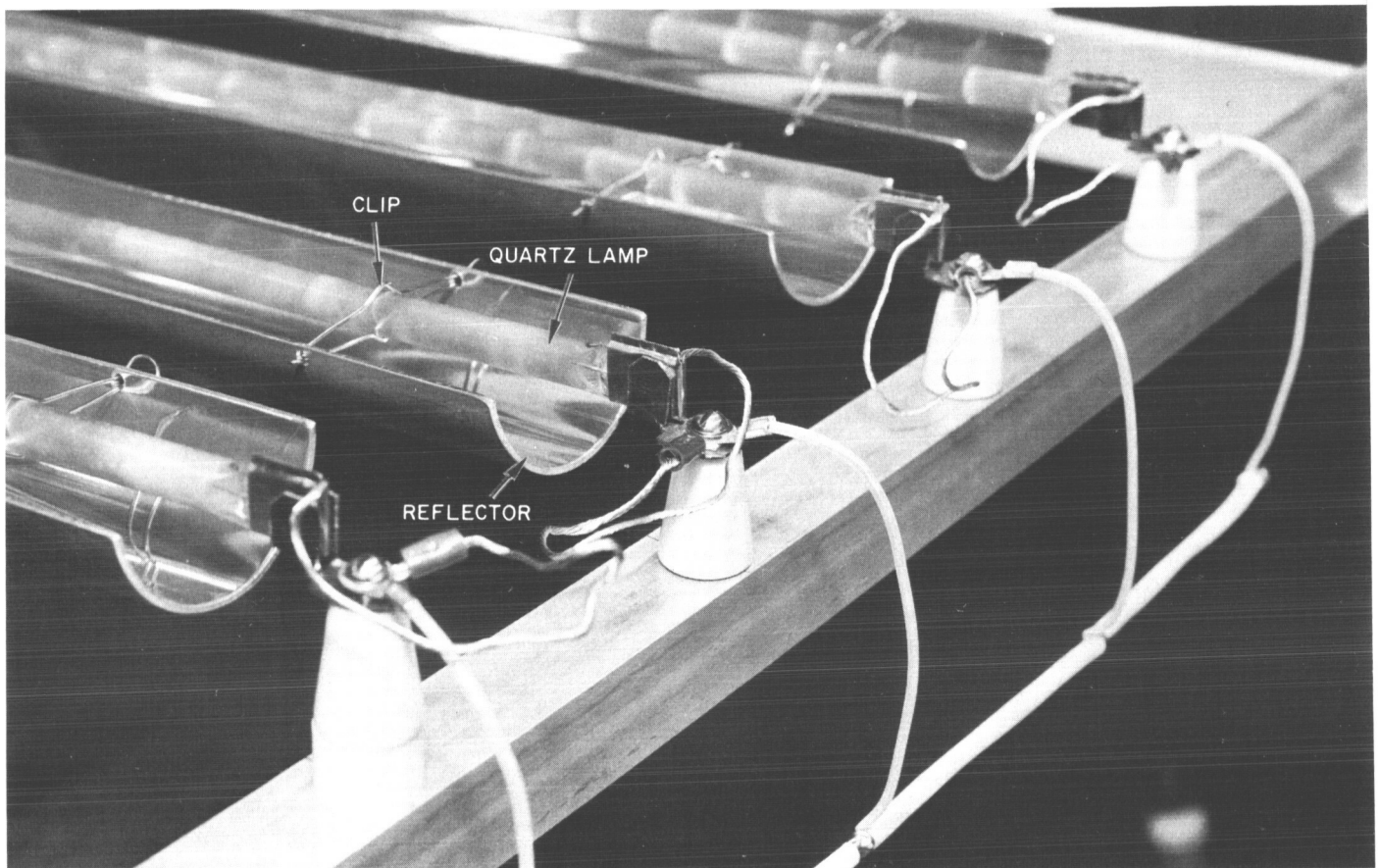

Fig. 3. Thermal radiation lamp bank